THE SPERM HEAD CYTOSKELETON OF THE PLAINS RAT (*Pseudomys australis*): A DEVELOPMENTAL AND COMPARATIVE STUDY

By

Dina Idriss

A thesis submitted to the Department of Anatomy and Cell Biology
in conformity with the requirements for
the degree of Master of Science

Queen's University
Kingston, Ontario, CANADA
August, 2001

ABSTRACT

Sperm head shape among eutherian mammals has been divided into two major types: spatulate (ie. bull sperm head shape) and falciform (ie. laboratory rat sperm head shape). The extensive cytoskeleton, or perinuclear theca (PT), of the Plains rat, *Pseudomys australis*, however, is greater than that of any other mammalian species studied. Not only does it have the falciform shaped apical hook (AH), or perforatorium, typical of many rodents, but it also has two falciform shaped ventral processes (VPs) which extend just inferior to the AH on its upper concave surface.

This investigation was designed to study the entire composition of the Plains rat sperm head perinuclear theca. First, we analyzed the composition of the VPs by isolating and alkaline extracting their cytoskeleton. Second, we examined the composition of the whole perinuclear theca of the Plains rat sperm head and the developmental aspect of these cytoskeletal proteins throughout spermatogenesis, particularly looking at spermiogenesis. Finally, we attempted to find a possible correlation between sperm head shape and a particular protein composition in the extensive cytoskeleton that occurs. The well studied bull and laboratory rat, along with their respective sperm head cytoskeletal proteins - bull-PT and lab rat-PERF - enabled us to use anti-sera raised against these two sets of proteins to analyze the Plains rat isolated sperm head VPs and extracted cytoskeleton compositionally and developmentally.

The compositional results of the isolated VPs indicated that material found within them is perforatorial-like and therefore similar to the material within the lab rat perforatorium; the dominant protein being PERF 15. As well, F-actin was immunoreactive in the VPs and not the AH of the mature spermatozoa. The alkaline

extracted Plains rat cytoskeleton revealed several proteins, the dominant one being a 15-kDa polypeptide, once again, similar to that of the lab rat sperm head PT protein profile. By immunoblotting, inter species cross-reactivity with antibodies raised against the whole bull-PT where shown to exist in the plains rat cytoskeleton. Immunocytochemical studies indicated that spatial and temporal development of PT and PERF proteins within the Plains rat spermatozoa revealed patterns similar to that seen in the bull and lab rat spermatozoa, respectively.

To further investigate sperm head shape we decided to look at an atypical rodent, *Bandicota indica*, which has a bulbous sperm head morphology. Interestingly, PERF proteins, which were thought to be found in falciform shaped sperm heads, were found in this spatulate shaped rodent.

In this study, we found that there is no correlation between PERF proteins and the falciform or hook shaped sperm heads due to its existence in the spatulate *Bandicota indica* as well as the presence of PERF in the AH and VPs after the shape has been formed. Furthermore, the presence of PT proteins within the cytoskeleton of all mammalian sperm heads appears to be fundamental due to their association with the developing acrosome throughout spermiogenesis.

I wish to dedicate this thesis to my parents
Samih and Sanya Idriss

And my brothers
Hassan and Wael Idriss

They have provided me with unconditional love
and support throughout all of my endeavors and dreams
and continue to do so relentlessly.

I also wish to dedicate this thesis in
the memory of my grandfather
Ibrahim Asphahani
who always believed in the everlasting
pursuit of education.

ACKNOWLEDGMENTS

I would like to first extend my appreciation to my supervisor Dr. Richard Oko who gave me the opportunity to work in his lab for the past three years. His support and dedication throughout this work has allowed me not only to expand my knowledge in this field of science but also to understand the true nature of work ethic, lab decorum and the real meaning of team-work. My time here at Queen's and in this lab will never be forgotten, I believe it was a time of self-improvement and I will forever benefit from this experience academically, socially, and personally. I would also like to extend my greatest appreciation to Dr.William G Breed from the University of Adelaide in Australia, for his help and collaboration in a large part of this work, he was an invaluable resource. I would like to thank Dr. Frederick Kan for his input and support throughout these few years. A big thank you to Dr. Stephen Pang, Dr. Micheal Kawaja, Dr. Conrad Reifel, Bob Temkin, Anita Lister, Marilyn McCauley, Brenda McPhail and the rest of the Department of Anatomy and Cell biology staff.

Yang Yu for her everlasting smile, constant support and superb technical assistance. Alma Barajas-Lopez and Gina Lam, you guys were wonderful to work with, thanks for all the help. To Ron Tovich, Alex Wu and Jeremi Mountjoy, being in the same lab with you guys for the past three years has been tons of fun. Jeson Sangaralingham, Karmen Krol, Perrie O'Tierney, Deborah McBride and Eugene Chung, thank you for all the laughs and talks, I'll miss those smiles in the hallways of the eighth floor. Rochard Beharry, thank you for being a great friend throughout these few years. And a huge thank you to all the wonderful friends in the department who have made this a great experience every step of the way. To Ritu Aul and Kate Angelis, I don't know what I would have done without your support, guidance and everlasting encouragement - I could go on forever (its not that much cheese, right?) – you guys were with me from the beginning and I will treasure this wonderful friendship forever. Diala Homaidan and Fareid Asphahani, my pseudo sister and brother, you two were there for me always – thank you!

To my best friend Mohammad Aoudeh- your spirit, drive and love have inspired me to push myself to so many limits. Thank you for always being there to make me laugh and encourage me when I needed it the most.

TABLE OF CONTENTS

LIST OF FIGURES

LIST OF ABBREVIATIONS

Ac.	acrosome
AH/AP	apical Hook/Process of falciform shaped sperm heads
Cyt.	cytoplasm
D	diplotene spermatocytes
ES	elongated spermatids
ER	equatorial region
F-actin	filamentous actin
FS	fibrous sheath
IAM	inner acrosomal membrane
L	leptotene spermatocytes
LM	light microscopy
MS	mitochondrial sheath
NaCl	sodium chloride
NaOH	sodium hydroxide
NE	nuclear envelope
OAM	outer acrosomal membrane
ODF	outer dense fibers
OPL	outer periacrosomal layer
P/MP	pachytene/mid- spermatocytes
PERF	referring to "perforatorial" proteins
PT	perinuclear theca (generally referring to the bull PT unless otherwise stated)
Pl	preleptotene spermatocytes
PS/PDL	post acrosomal sheath/post acrosomal dense lamina of PT
SA	Separated acrosomal head segments (a part of the acrosome separates and is found in the VPs of the plains rat)
SDS-PAGE	Sodium Dodecyl-sulfate Poly-Acrylamide Gel Electrophoresis

Sg.	spermatogonia
SL	subacrosomal layer of the PT (also known as Perforatorium in falciform murids)
TBS	tris-base saline buffer
TEM	transmission electron microscopy
VPs	ventral processes of the Plains rat
VS	ventral spur
Z	zygotene spermatocytes

1. GENERAL INTRODUCTION

I. CLASSIFICATION

One of the most exciting aspects of this study is the realization that unexplainable evolutionary processes have a great impact on the diversity of male reproductive anatomy and physiology. To appreciate the development of the male reproductive anatomy that has evolved between species requires some basic knowledge of inter-relationships between species and their evolution.

The five-Kingdom system recognizes two types of cell: prokaryotic and eukaryotic. The five Kingdoms are Monera (which includes all the prokaryotes - bacteria and cyanobacteria), Protista (unicelluar forms in majority, with some simple multi-cellular forms), Plantae, Fungi, and Animalia (reviewed by Campbell, 1987). The order of classification is as follows: Kingdom, Phylum (subphylum), Class (superclass, infraclass), Order, Family, Genus, and Species (Hickman and Roberts, 1994).

Of great interest to this project is the Kingdom Animalia with which are many phyla. Here I will concentrate on a number of the Class Mammalia that occur in the subphyla vertebrata. All mammals are characterized by having a four-chambered heart, a diaphragm dividing the upper chest from the rest of the body, insulating hair, and the occurrences of lactation (Keaton and Gould, 1993). This Class is divided into three infraclasses. The first is the Monotremata (prototheria) where species lay eggs but secrete milk and the only living monotremes being the echidna (also known as the spiny anteater) and the duck-billed platypus (Bedford, 1991). The second infraclass is the Marsupialia (also known as Metatheria) which carry the fetus in the uterus for a brief

period and then the young continue development attached to a nipple in the abdominal pouch of the mother (Bedford, 1991). The final infraclass is the Eutheria (also referred to as Placentals as they have a well developed placenta) within which 17 different Orders occur; species in the Order Primates (humans), the Orders: Rodentia (mice and rats) and Artiodactyla (bull) (Hickman and Roberts, 1994) are included in this thesis. Specific reference to the particular genus and species of the animal used will be mentioned throughout the text when necessary.

There are differences between eutherians in sperm head morphology as well as between the other two mammalian infraclasses – marsupials and montremes. The head of the spermatozoon in eutherian mammals includes disulfide bonding between chromatin fibers, an equatorial segment of the acrosome and bilateral flattening (reviewed by Breed, 1997). The two most studied and established models of spermatozoa head and tail anatomy and protein composition in our lab are the laboratory rat and the bull.

II. THE MAMMALIAN SPERMATOZOON

The spermatozoa and oocyte of a species coevolve structurally with the ultimate goal of gamete fusion. The eutherian oocyte is very small, with a prominent zona pellucida (ZP) while marsupial and monotreme oocytes have larger eggs and markedly smaller ZPs. With the emergence of disproportionate growth of egg vestments in eutherians, new structural features have coevolved in the sperm head to help the penetrating spermatozoon (Bedford, 1991). Thus, the study of gamete interaction in eutherian animal for gaining insight into the understanding of mechanisms involved in mammalian fertilization.

The male gamete, with its haploid DNA, is a highly specialized cell that undergoes a series of morphological and biochemical changes, in a process known as spermatogenesis, to become viable for the fertilization process (Reviewed by Eddy and O'Brien, 1994). There are two main components of the spermatozoon: the head and the tail. Early on in spermiogenesis, the last phase of spermatogenesis, the sperm head nucleus becomes condensed to protect the genetic material from insult during its journey to the oocyte. The sperm tail, which begins to develop a little later in spermiogenesis than the head, provides the motile force that allows the sperm to fertilize. Spermatozoa must first travel through the male reproductive tract, and then through the female tract to reach the haploid oocyte at the site of fertilization, producing a diploid cell destined to become an embryo (Reviewed by Eddy and O'Brien, 1994)

(i) Tail Structure

The sperm tail is divided into four distinct segments. The axoneme is a structural component of the sperm tail that extends the full length of the flagellum and is composed of a "9 + 2" arrangement of microtubule doublets. The mitochondrial sheath (MS) encircles the middle piece under the sperm head plasma membrane and provides energy source for tail movement. The outer dense fibers (ODFs) are cytoskeletal structures which run the entire length of the tail. In the middle piece of the tail, there are nine ODFs each associated with a microtubular doublet of the axoneme. In the principal piece, the ODF are reduced to seven and decrease in size distally. The fibrous sheath (FS) surrounds the ODF in the principal piece of the tail and is composed of longitudinal columns and numerous transverse ribs that bridge the longitudinal columns on either side. The sperm tail implants into the head of the spermatozoon at the connecting piece (Fawcett, 1965, Zamboni and Stefanini, 1971).

(ii) Sperm Head: Nucleus and Associated Structures

Diversity among the sperm head of eutherian species is prevalent in terms of shape and size. There are two major shapes: spatulate and falciform. Spatulate shaped sperm heads are characteristic of most mammals including primates (eg. bull, monkey and human). Falciform shaped spermatozoa are characteristic of many rodent species including hamster, mouse and rat (Clermont and Leblond, 1955; Fawcett, 1970). The divergence of sperm head shapes during evolution likely reflects the differences in gamete function during fertilization (Bedford, 1991).

In most species, the nucleus of the spermatozoon constitutes the major portion of the head. It is surrounded by a double membraned nuclear envelope that is devoid of nuclear pores (reviewed by Fawcett, 1975) except at its basal region. The nuclear contents of the mature spermatozoon consist of highly condensed chromatin that remains inactive until post-fertilization events. This DNA retains its compact and condensed form by associating with highly basic cytsteine-rich nuclear proteins termed protamines (Balhorn *et al.*, 1984; Loir and Lanneau, 1984; Hecht, 1987.).

The acrosome is an enzyme-filled sac covering the apical portion of the sperm head. It extends caudally to make up the equatorial segment; a rigid-band encircling the mid-section of the sperm head. The acrosome is encased in a membrane that is regionally divided into the inner and outer acrosomal membranes. The outer acorsomal membrane (OAM) underlies the plasma membrane of the spermatozoon and the inner acrosomal membrane (IAM), which lies between the acrosomal contents and the perinuclear theca (PT).

III. PERINUCLEAR THECA

The perinuclear theca (PT) is a rigid cytoskeletal capsule that covers the sperm nucleus except where the tail implants into the head (Oko, 1997). Due to species differences in sperm head shape, the PT also displays species-dependent structural and regional variances. Apically, it resides between the inner acrosomal membrane (IAM) and the nuclear envelope (NE), forming the subacrosomal layer (SL). Caudally, it lies between the sperm plasma membrane and the nuclear envelope, forming the postacrosomal sheath (PS). Compositional studies of the perinuclear theca structure done in the bull (Clermont and Leblond, 1955; Olson and Winfrey, 1988; Oko and Maravei, 1994; Oko, 1995) and in the rat (Olson *et al.*,1976; Oko *et al.*,1990; Oko and Clermont, 1991; Oko,1995) have demonstrated similarities, and while the sperm heads of these two species are structurally diverse many of their PT proteins appear to be evolutionarily conserved (reviewed by Oko, 1995).

(i) The Bull Perinuclear Theca Composition

The majority of species within the class of eutherian mammals (eg. man, monkey, and bull) have spatulate shaped sperm heads (Breed, 1997). Bovine provides an excellent model for this study of spatulate shaped sperm heads. The bull PT has been described extensively and it is found between the acrosome and nucleus forming the subacrosomal layer (SL) (Oko and Maravei, 1994). It also extends caudal to the acrosome forming the postacrosomal sheath (PS) and hence completely encases the nucleus except at the implantation fossa. (Oko and Maravei, 1994). The bull PT is structurally and

compositionally continuous with the outer periacrosomal layer (OPL) which is located between the outer acrosomal membrane and the sperm plasma membrane, overlying the equatorial segment of the acrosome (Reviewed by Oko *et al.*, 2001; Oko *et al.*, 1990; Oko and Maravei, 1994; Oko, 1995). Analysis of the protein composition of bull PT has revealed six prominent polypeptide of molecular weights, 60-, 36-, 32-, 28-, 24-, and 15-kDa. Immunolocalization of these proteins has revealed that the 15-kDa polypeptide is exclusively subacrosomal while the remaining five, including the 60-kDa, reside throughout the PT (Oko and Maravei, 1994), suggesting a regionally variant PT protein composition (Oko *et al.*, 1990). Of these six PT proteins, only two have been identified and characterized at the molecular level. The 60- kDa PT protein was identified as calicin, an actin binding protein belonging to the kelch family (Von Bulow *et al.*, 1995; Lecuyer *et al.*, 2000). The 15- kDa PT protein has been recently identified as a novel subacrosomal H2B variant (SubH2Bv) that has a postulated role in acrosomal-nuclear docking during spermiogenesis (Aul and Oko, in press).

(ii) The Laboratory Rat Perinuclear Theca Composition

The most extensively studied model of the falicform sperm head shape is the laboratory rat. The perinuclear theca in falciform shaped heads of spermatozoa has structural differences as well. The subacrosomal layer (SL) extends apically beyond the nucleus and it is referred to as the perforatorium. Unlike the SL of bull PT, the perforatorium is a curved pointed structure, which is triangular in cross-section over the apical half and beyond the tip of the nucleus (Lalli and Clermont, 1981, Oko and Clermont, 1988). Protein composition of the isolated PT, which includes both the

perforatorium and the PS, show an almost identical pattern to that described in the bull with a 15-kDa polypeptide predominating over the other bands (refer to Appendix A) (Oko and Clermont, 1988; Oko *et al.*, 1990, Oko and Maravei, 1994; Oko, 1995). This protein is localized to the perforatorium exclusively and was termed PERF 15. PERF 15 was cloned and its cDNA sequence revealed that it shares extensive amino acid sequence similarities with a family of lipid binding proteins including myelin P2, adipocyte lipid-binding protein, and heart, liver and intestinal fatty acid binding proteins (FABP) (Oko and Morales, 1994; Pouresmaeili *et al.*, 1997). Of all these proteins, PERF 15 displays the greatest homology to myelin P2, with 60% amino acid similarity. Myelin P2 exists between opposing membranes in the myelin sheath of Schwann cells. PERF 15 resides between the IAM and the nuclear envelope, and is therefore thought to be involved in the mediation of binding of these membranes in rat spermatozoa (Pouresmaeili *et al.*, 1997).

The ventral spur (VS) is situated directly against the nucleus and exists just below the lower ventral concave surface of the lab rat falciform sperm head as a triangular extension of the postacrosomal sheath (Oko *et al.*, 1990). It is composed of the same proteins that are found in the perinuclear theca. The cortex of the VS is composed of polypeptides that are found in the postacrosomal sheath of the PT (the region delineated by yellow in Fig 1a), while the core region is composed of proteins found in the perforatorium of the PT (the region delineated by red in Fig 1a) (Oko *et al.*, 1990).

(iii) Comparison of The Perinuclear theca in the Bull and Rat

Selective alkaline extraction of PT proteins in the bull and rat and comparison of the molecular weight of these polypeptides has shown very similar profiles (see

Appendix A). However, differences arise when examining the regional composition of the bull and rat PT. To explore the similarities between the two species, antibodies raised against the *whole bull PT extract*, as well as against its six major proteins, were used to analyze the alkaline extracted *whole PT of the rat*. This resulted in a cross-reaction between the bull-PT antibodies and the rat PT blot in all cases examined (Oko, 1995). Studies showed the sharing of epitopes between the PT 15 and the PT 60 polypeptides of bull and rat PT, which suggested that protein constituents of the PT are conserved between species (Oko 1995). The isolated *rat perforatorial* profile, on the other hand, was different from that of the *entire bull PT* profile because of its lower number of evident polypeptides; the prominent ones being 34- and 15-kDa polypeptides (Oko, 1988; Oko, 1995). The major protein found in the isolated and extracted perforatorial polypeptide profile was the 15-kDa protein PERF 15, the predominant protein of the entire rat PT extract (Oko and Clermont, 1988).

The species differences in PT structure are important to recognize when studying the conservation of these proteins. For example, the bull SL region cannot be isolated on its own because it is tightly adhered to the nucleus and does not have an extended portion. The perforatorium which extends from the SL of the lab rat and mouse, beyond the tip of the nucleus and therefore can be easily separated. Consequently, PT composition and localizational comparisons that have been carried out between the bull and rat SL regions are only via immunocytochemical studies. As well, PT-antibodies were raised from the bull PT proteins and not the lab rat because additional perforatorial proteins predominate in the rat sperm head cytoskeleton. For these reasons, antibodies raised against the bull sperm head PT proteins are used to study the rat sperm head PT.

To compare falciform and spatulate head shapes, it is important to first examine the differences that are found within the subacrosomal layer of both, the region in which drastic species specific sperm head changes occur; the falciform shaped sperm head has a larger extension of the cytoskeleton than the spatulate. The antibodies previously raised against the entire-bull PT and those against the entire-rat perforatorium, immunocrossreact with *bull-PT* and *rat-PERF* proteins, respectively. Antibodies affinity purified and directed against specific proteins of either the bull sperm head PT or the lab rat perforatorium have shown similarities in developmental and localization with their corresponding group of proteins (Reviewed by Oko, 1995). Therefore, to avoid redundancy and confusion, only the following two specific proteins, PT 15/SubH2Bv and PERF 15, were used to represent each set of proteins in immunocytochemical studies

In order to study and understand the proteins which compose lab rat and bull perinuclear theca and the probable association with their species specific shape, a description and comparison of their developmental expression is needed. But before specific details of PT protein expression are examined, a more detailed explanation of the development of mammalian spermatozoa will provide a basis for understanding specific references to mammalian spermatogenesis.

IV. SPERMATOGENESIS

The primordial germ cells originate from the yolk sac to colonize the gonad during embryonic development before sexual differentiation (Evrett's review, 1945; Mintz, 1959). In mammals the sex cords have two types of cells, the gonocytes and the somatic cells, the former of the two gives rise to the spermatogonia (Mintz, 1960; Courot *et al.* review, 1970).

The male gamete is a highly specialized cell that undergoes a series of morphological and biochemical changes to become viable for the fertilization process. Spermatogenesis is the process through which male mammalian germ cells undergo in order to become mature haploid celled spermatozoa (Courot *et al.* review, 1970). Its general organization is the same in sequence. First is the mitotic phase in which spermatogonia stem cells prolilferate and differentiate into spermatocytes, second is the meiotic phase which yield the haploid spermatids and the last phase is spermiogenesis, a morphogenic process producing highly specialized spermatozoa. (Courot *et al.* review, 1970; Clermont *et al.*, 1993).

(i) Mitosis

During the mitotic phase, the spermatogonial cell population undergoes numerous proliferations to build a large population of cells. Furthermore, it maintains enough cells in reserve that do not become committed to development in order to allow spermatogenesis to become initiated regularly (Russell *et al.*, 1990). There are three types of spermatogonia: stem cell, proliferative, and differentiating spermatogonia. The resistant stem cell spermatogonia serve as a potential repopulating source of germ cells in case of serious insult to the testis. The mechanism by which stem and proliferative spermatogonia transform into differentiating spermatogonia in both the bull (reviewed by Barth and Oko, 1989) and the lab rat (Ewing *et al.*, 1980) is still not completely clear, however both provide sufficient understanding for our application during developmental analysis of the sperm head cytoskeletal proteins. The following description of mitosis is

an adaptation of both the rat and bull models which generally follow the same description.

Type A spermatogonia are the germ cells that rest on the basal lamina and there are generally four types, A_0, A_1, A_2 and A_3. The Ao spermatogonia give rise, through mitosis, to either A_1 (renewing stem cells) and A_0 (reserve stem cell) (reviewed by Barth and Oko, 1989). In mammals, type A spermtogonia can be divided into dark and pale types on the basis of nuclear staining in light and electron microscope studies (Burgos et all, 1970; Clermont, 1972; Zamboni, 1971). The dark type-A are considered to be reserve stem cells (ie. A_0), while the pale type-A are renewing stem cells which are more differentiated and result in intermediate spermatogonia (ie. A_1). The renewing stem cells were found to originate after the mitosis of the A_2 type, which was an equivalent mitosis resulting in A_1 and A_3 spermatogonia (reviewed by Barth and Oko, 1989). Thus at a particular stage (X in bull and XIII in rat), two populations of A spermatogonia are found in the basal layer of the seminiferous tubule, A_1 which renews the spermatogonial line in Stage 1 and A_3 which goes on to become intermediate spermatogonia. B_1 spermatogonia, which are mitotically derived from the intermediate type, divide again to form B_2 spermatogonia which eventually divide and become preleptotene spermatocytes (Amann, 1962; Berndtson, 1978; reviewed by Barth and Oko, 1989). By microscopy, the different types of spermatogonia can be distinguished from one another by the amount of chromatin lying along the inner aspect of the nuclear envelope; Type A display essentially none, intermediate spermatogonia have a moderate amount and Type B posses a large amount (Reviewed by Russell, 1990). This sequence of spermatogonial divisions

[A_0, A_1, A_2 A_3, Intermediate, B_1 ,B_2] leads to type B mature spermatogonia which can then enter the next phase of spermatogenesis.

(ii) Meiotic Phase

During the two cellular divisions that make up the meiosis phase, chromosomes are recombined and genetic material is halved in each cell. The number of germ cells is therefore quadrupled after the completion of this phase. During the first meiotic division, prophase is an extensive process and the nuclear changes that occur are the morphologic basis for dividing the spermatocytes. Prophase I consists of (Russel et al review, 1990):

Preleptotene (Pl) ------ Leptotene (L) ------Zygotene (Z) ------ Pachytene (P) ------ Diplotene (D) ----- (Diakenesis)

The preleptotene spermatocytes (Pl) is a result of the last mitotic division of a spermatogonia. Leptotene cells signal the initiation of the meiotic prophase; their nuclei gradually lose peripheral chromatin and form fine unpaired threads. As this transition occurs, their nuclei are more rounded and they move slightly away from the base of the seminiferous tubule (Russell, 1977, 1978). In zygotene (Z) cells, homologous chromosomes have become paired, which distinguishes them from the (L) by their thicker appearance (Moses, 1968). In pachytene spermatocytes (P), the chromosomes have become fully paired and crossing over occurs at this time, as well, they grow rapidly in size (Russell and Frank, 1978), their nucleoli enlarge greatly and the sex chromatin is visible (Solari, 1968; Solari and Rres, 1967). Late pachytene (P) spermatocytes are ovoid in comparison to early pachytene (EM) and mid pachytene (MP). The diplotene (D) phase is brief and it is at this time that the chromosomal pairs separate from each other

except at the chiasmata. After the formation of the diplotene spermatocytes, the remainder of the first meiotic division (meiosis I) is completed as the primary spermatocytes continue through metaphase, anaphase and telophase, rendering secondary spermatocytes (Russell and Frank, 1978). The second meiotic division (meiosis II), "reductional division", follows rapidly to produce haploid spermatids. Meiosis II cells can be distinguished form meiosis I cells based on their relatively smaller size, furthermore, all the meiotic II phases are brief, including the prophase (Russell *et al.* review, 1990).

(iii) Spermiogenesis

It is throughout this last phase of spermatogenesis that the spermatid undergoes morphologic changes to form a mature spermatozoon. This process can be divided into steps according to the structural features that develop and vary among species. Appendix B is a detailed description of the spermiogenic steps that are grouped into four phases: the Golgi phase, the cap phase, the acrosomic phase and the maturing phase in the (i) rat and (ii) bull.

(a) Development of the Acrosome, Nuclear Elongation and Nuclear Condensation

Early in spermiogenesis, spermatids contain proacrosomic granules, rich in glycoproteins which are formed on the trans-face of the Golgi stacks. These granules become membrane enclosed proacrosomic vesicles that eventually coalesce to form a single granule known as the acrosomal vesicle. This is rounded in shape until it becomes associated with the nuclear membrane. Upon attachment to the nuclear envelope, the

acrosome flattens and spreads over the nucleus. The Golgi apparatus is closely positioned and continues to contribute more material to the developing acrosome via small carrier vesicles, causing the lighter portion of the acrosomic system to expand at the surface of the nucleus and the developing acrosome to take the shape of a cap over it (Leblond and Clermont, 1952; Lalli and Clermont, 1981; Russell *et al.*, 1990). The tight adhesion of the acrosomal membrane to the nuclear envelope is thought to be due to the intervening perinuclear theca, that later condenses to form part of a rigid capsule that covers the nucleus of the spermatozoa (Oko review, 1995). The spermatid nucleus moves to the cell surface and this region becomes tightly opposed to the cell membrane, causing polarity to the cell and signaling segregation of the head (anterior) region from the tail (caudal) region. At this point, the Golgi apparatus separates from the acrosome and ceases to contribute glycoproteins, it later regresses and disappears from the cytoplasm (Barth and Oko, 1989). At this time, the nucleus begins to take its species-specific shape (falciform in rat or spatulate in bull) as it elongates. The acrosomal shape changes may be passively related to the nuclear elongation occurring at the same time, or due to the activity of the actin present in the PT region during development (Russell *et al.*, 1986).

Another major event in spermiogenesis is nuclear chromatin condensation where two main sequential stages of chromatin reorganization are observed: (1) the first stage describes a remodeling of chromatin from its normal nucleosomal form to a threadlike filamentous form, and (2) in the second, the chromatin filaments thicken, become coarse, and aggregate into compact masses that coalesce to form a dense chromatin mass (Oko *et al.*, 1996). By the final stages of spermiogenesis, the chromatin mass condenses to give a homogenous chromatin and filaments can no longer be resolved. The transformation to

the filamentous form of chromatin has been correlated with a modification or loss of nuclear histones while its progressive condensation into the compact form is thought to be influenced by the presence of spermatid nuclear proteins, Transition Proteins (TP1 and TP2) (Meistrich *et al.*, 1994, Oko et al, 1996). Lastly, these transition proteins are replaced late in spermiogenesis by protamines marking the final chromatin condensation (Hecht, 1989). Simultaneously to this entire process, sperm tail formation occurs caudally.

(b) Formation of the Sperm Tail

Formation of the tail begins in early steps of spermiogenesis as a pair of centrioles migrate toward the nucleus and solidly bind to it. The distal centriole triggers the growth of the axoneme while the proximal centriole is associated with the formation of the capitulum, a structure that anchors the proximal end of the striated columns in the connecting piece (Fawcett, 1975). The nine ODFs develop in a proximal to distal direction in association with the axoneme starting early in spermiogenesis and enlarging in its final phase, as they stretch the length of the sperm tail (Irons and Clermont, 1982a; Oko and Clermont, 1990; Barth and Oko, 1990; Clermont *et al.*, 1993 and Oko and Morales, 1996). The FS develops in a distal-to-proximal manner along the axoneme beginning early in spermiogenesis until mid-maturation (Irons and Clermont, 1982b; Barth and Oko, 1990). The mitochondrial sheath assembly is initiated just after the annulus descends to form the midpiece-principal piece junction in the maturation phase. The mitochondria are located peripherally in early spermatids and following the sliding of the annulus along the axonemal complex, they line up along the ODFs between the

neck and annulus. Later in spermiogenesis, they condense, take a tubular-crescentric shape and align themselves side by side in a spiral manner, demarcating the middle-piece of the tail (Irons, 1983; Otani *et al.*, 1988). Just before spermiation, with the sperm head and tail fully formed, the residual body of the midpiece is extruded at the level of the connecting piece. The final post-testicular maturation process takes place in the epididymis (Barth and Oko, 1990).

V. DEVELOPMENTAL EXPRESSION OF THE PERINUCLEAR THECA IN BULL AND RAT

Studies of the developmental expression of bull-PT proteins and rat-PERF proteins have been carried out (Oko and Clermont, 1991; Oko and Maravei, 1995), however, a developmental comparison between the two species has not. It is important to distinguish between rat-PERF and rat-PT proteins because detailed immunohistological studies on the former (Oko *et al.*, 1990; Oko and Clermont, 1991) but not the latter are available. In fact, this is the rationale for pursuing the study of PT protein expression in falciform shaped sperm head, using the anti-bull PT antibodies as probes. First, however, a detailed comparison of bull-PT protein and rat-PERF protein expression is required.

The spatial and temporal distribution of bull PT protein expression by immunocytochemical analysis (Oko and Maravei, 1995) was restricted to the spermatid population. During the Golgi phase, PT proteins surround the hydrolytic enzyme-filled proacrosomic vesicles, which fuse to become the forming acrosomic vesicle (Thorne-Tjomsland *et al.*, 1988). The acrosomic vesicle, surrounded by PT proteins, then becomes firmly anchored to the nucleus during development in the process known as acrosomal-

nuclear docking. During the capping phase, as the acrosomic vesicle spread over the nucleus PT proteins continue to surround the entire vesicle as well as within the cytoplasmic region corresponding to the subacrosomal layer. At the end of the capping phase, during the acrosomal phase and throughout the maturational phase, PT proteins are no longer seen to surround the acrosome in association with the plasmalemma. At this point they are: (1) overlying the outer periacrosomal layer in the equatorial region, (2) underlying the acrosome in the subacrosomal layer and (3) lining the postacrosomal sheath (Oko and Maravei, 1995). PT 15 (SubH2Bv) is the only bull-PT protein found to be restricted to the subacrosomal region of the sperm head PT so far (Oko and Maravei, 1995; Aul and Oko, in press).

Immunocytochemical studies of rat testicular sections reacted with antibodies raised against the PERF 15 and against the whole rat peroforatorium, were identical except for regional variation of labeling seen in the last step of spermiogenesis (Step 19). PERF 15 is first seen in nucleus and cytoplasm of pachytene spermatocytes, with an increased expression as development continues. In mid-spermiogenesis, it is diminished in the nucleus and increased in the cytoplasm. Immunocytochemical analysis of PERF proteins during development has shown that at step 12-13 of spermiogenesis, aggregates of PERF begin to appear, suggesting condensation of the perforatorial network. During the maturation phase, the perforatrium in the spermatid head begins to form its characteristic falciform shape along with the nucleus and acrosome. In the last step of spermiogenesis, step 19, the perforatorium is formed with the condensation of perforatorial material. In the mature rat spermatozoa there is regional differences in perforatorial protein composition. The majority of PERF proteins are found throughout

the entire perforatorium and the inner aspect of the ventral spur, while PERF 15 appears localized to the thicker apical portion of the perforatorium and the ventral spur but not to the narrower caudal part underlying the head cap (Oko and Clermont, 1991). Interestingly, PT60 (calicin) was studied in the lab rat and its developmental expression was found to be the same as the bull PT proteins (Oko and Clermont, 1991a, 1991b). It was the first example of the two groups of proteins present within the one species, the lab rat perinuclear theca.

It is evident that these two sets of proteins, PERF and PT, behave quite differently in developmental localization and assembly pattern throughout the cycle of the seminiferous epithelium. This difference would be interesting to resolve in more detail within one particular species, *Pseudomys australis*, which possesses a cytoskeleton greater and perhaps more complicated than any other mammalian species. Furthermore, the concept of PERF vs. PT proteins and their association with falciform and spatulate shaped sperm heads can be further understood.

VI. *PSEUDOMYS AUSTRALIS* (PLAINS RAT): A Model for The Study of Sperm Head Perinuclear Theca Protein Composition, Development and Shape

Current taxonomic classification place the Plains rat, *Pseudomys australis* as a native Australian murid, of the *Pseudomys* genus which belongs to the Conilurini tribe of the subfamily Hydromyinae. It has evolved, along with the laboratory rat, 20 million years ago from one ancestral form (Lee *et al.*, 1981).

The Plains rat has a distinctive sperm head structure which, in addition to possessing the apical hook similar to that of the laboratory rat, has evolved two elaborate processes known as ventral processes (VPs) extending from the upper concave surface of

the sperm head (Fig.1b) (Breed, 1983). It is interesting to note that other several species of rodents of the same genus have different head shapes and this is seen very clearly in the genus *Pseudomys* where one species has the three-hooked sperm head while another does not (Breed, 1983).

It has been suggested that the VPs are a result of increased barriers to sperm penetration. Thus, natural evolutionary processes as well as a possible decrease in penetration barriers have resulted in some Hydromyinae retaining the VPs while others, close in evolutionary relation, have not (Flaherty, 1987; Breed, 1983, 1984) Furthermore, they may have evolved to protect the cell membrane overlying the equatorial segment as they form a larger penetration slit in the zona pellucida, facilitating the passage of the spermatozoa (Bedford, 1982, 1983).

The VPs were first described as having the following compositional characteristics: (1) a core of electron-dense material confluent with the material in the subacrosomal space, (2) a peripheral layer of unknown origin and (3) the presence of actin within their core (Flaherty *et al.*, 1983). The two regions of material were later characterized as subacrosomal material in the core and as a continuation of the postacrosomal sheath in the cortex (Flaherty and Breed, 1987). In the lab rat or mouse, there are actin filaments present during spermiogenesis, however, they are lost or depolymerize before the sperm reach the epididymis (Lora-Lamia *et al.*, 1986). Interestingly, actin filaments are detected in the mature plains rat VPs and not the AH (Flaherty *et al.*, 1983). During step 13 of spermiogenesis in the Plains rat, the VPs undergo a change in degree of curvature, flattening and shape. These changes are thought to be due to actin since they only occur after appearance of actin filaments (Breed and

Leigh, 1991). However, to understand the mechanism behind these shape changes, it is important to first identify the entire composition of these VPs.

This particular study was initially designed in order to investigate the possible link between sperm head shape and a particular protein composition in the extensive cytoskeleton that occurs. It has become recently evident that PERF proteins are unique to the rodent falciform shape, thus, one could hypothesize that these proteins are involved in sperm head shaping. To further investigate this theory and substantiate what has already been shown in terms of spatulate versus falciform PT composition, a unique Australian rodent - *Pseudomys australis* - was selected which has a more extensive development of the cytoskeleton than any other mammalian species studied.

As an addition to this study, we decided to investigate the sperm head of a rodent species from Southern Asia which has an unusual morphology and structural organization. The sperm heads of *Bandicota indica* are bulbous or globular in shape and have no narrow uniformly defined apex of a delineated perforatorium (Breed *et al.*, 1993) (Appendix C).

HYPOTHESIS AND OBJECTIVES

The underlying hypothesis of my thesis is that the composition and developmental assembly of the proteins found in the Plains rat extensive sperm head cytoskeleton, the perinuclear theca, will be similar to what has been found in the laboratory rat sperm head cytoskeleton. Furthermore, we hypothesize a correlation between the falciform shaped sperm head perforatorial (PERF) proteins found in rodents, which are not found in spatulate shaped mammalian sperm head cytoskeleton, and the falciform shape that occurs. To test this hypothesis, we look at the extensive falciform shaped cytoskeleton of the Plains rat as a model and compare it with the classical falciform shaped sperm head of the lab rat and spatulate shaped sperm head of the bull.

Objectives:

1) To isolate and then analyze the protein composition of the Plains rat, *Pseudomys australis*, ventral processes (VPs).
2) To analyze the protein composition of the alkaline (NaOH) extracted plains rat perforatorial-perinuclear theca (PERF-PT) complex.
3) To evaluate the expression and assembly pattern of PERF versus PT proteins during spermiogenesis in the Plains rat.
4) To compare the cytoskeletal, or perinuclear theca, compositions and developmental expression patterns of PERF and PT in the Plains rat with that of (a) the falciform shaped sperm head of the laboratory rat and (b) the spatulate shaped sperm head of the bull and the rodent, *Bandicota indica*.

CHAPTER 2

THE PROTEIN COMPOSITION OF THE VENTRAL PROCESSES FOUND ON THE SPERM HEAD OF THE AUSTRALIAN HYDROMYINE RODENT *PSEUDOMYS AUSTRALIS*

ABSTRACT

The sperm head of the plains rat, an Australian hydromyine rodent, is highly complex in structure and contains in addition to an apical hook, two large ventral processes (VPs) that extend from the upper concave surface of the sperm head just below a larger apical hook (AH). They are known to be an extension of the sperm head cytoskeleton (also known as the perinuclear theca (PT)) surrounded by postacrosomal dense lamina. The major focus of this study is to determine the protein composition of these ventral processes. We isolated the VPs from the entire sperm head, the proteins within them were separated by SDS-PAGE, and then probed with antibodies raised against the laboratory rat perforatorial and bull perinuclear theca sperm proteins. The same antibodies were used to determine the perforatorial and perinulcear theca proteins by immunogold labeling of transmission electron microscopic sections. The results indicate that the VPs are largely composed of perforatorial cross-reacting proteins together with F-actin, with the major protein being PERF 15. The perinuclear theca proteins are, by contrast, confined to the periphery of the acrosomal and nuclear membranes. In conclusion, this study has shown that the VPs of the spermatozoa of Australian Hydromine rodents are perforatorial-like appendages that contain similar proteins to the perforatorium of the apical hook along with F-actin. The functional significance of these specialized processes remains unknown.

INTRODUCTION

Most species of eutherian mammals have a spatulate, or pear-shaped, sperm head that is mainly composed of a nucleus with highly condensed chromatin. Over the anterior two thirds of the nucleus an acrosomal cap exists that contains hydrolytic enzymes most of which are released at the time of the acrosome reaction. Between the inner acrosomal membrane and outer nuclear envelope a space is present, the subacrosomal layer, that contains several proteins whose function may be to attach the inner acrosomal membrane to the outer nuclear envelope. This space extends posterior to the acrosomal cap where it gives rise to a postacrosomal sheath from which electron-dense material extends to, and stabilizes, the overlying plasmalemma.

Common laboraotry rodents, such as the Norwegian rat, differ in head shape from other mammals; they have a falciform or hooked sperm head. They may have similar structural components to the already described paddle-shaped sperm heads, but they highly differ in both organization and composition. In these spermatozoa the nucleus extends to the apical hook where it is surrounded by a large extension of the cytoskeleton that is generally referred to as the perforatorium (Friend, 1978; Bishop and Austin, 1957; Bishop and Walton, 1960; Piko, 1969; Clermont *et al.*, 1955). Early studies on the protein composition of the perforatorium suggested that it was primarily composed of a single 15- kDa protein (Olson *et al.*, 1976), but subsequently it has been shown to contain several proteins whose composition differs somewhat from the postacrosomal sheath with which it is continuous (Oko & Clermont, 1988; Oko and Moussakova, 1990; Oko, 1994). The 15 kDa protein present within the rat perforatorium has been recently cloned and

characterized as novel testicular protein and termed PERF 15 (Oko& Morales, 1994; Pouresmaeili *et al.*, 1997; Korley *et al.*, 1997).

Most Australian Hydromine rodents have a sperm head structure that is considerably more complex than the laboratory rat. In addition to the apical hook (AH) already described, there are two processes which extend from its upper concave surface termed ventral processes (VPs) (Breed and Sarafis, 1979). Studies carried out on the VPs have shown them to develop in late spermiogenesis and are largely composed of electron-dense material that is continuous with the perforatorium of the AH (Breed, 1983, 1984,1997; Flaherty, 1987; Flaherty and Breed. 1983, 1987). The chemical composition of these processes is largely unknown although filamentous actin has been shown to be present (Breed, 1997; Flaherty, 1987; Flaherty and Breed, 1987; Flaherty *et al.*, 1983; Breed and Leigh, 1991) that is not present in the perforatorium of mature the sperm head of the laboratory rat (Oko *et al.*, 1990; Fouquet *et al.*, 1989; Russell *et al.*, 1986). In this study we isolate the VPs and determine their protein composition by SDS-PAGE and Western blotting using antisera raised against the perforatorium of the laboratory rat and the perinuclear theca of the bull. The same antibodies are then used for immunogold labeling, via TEM, which can localize any cross-reacting proteins on the Plains rat testis and epididymal sections.

MATERIALS AND METHODS

The species of hydromyine rodent used in this study is the plains rat, *Pseudomys australis*. This species has a sperm head morphology typical for this subfamily of murid rodents that contains both an apical hook and two VPs described above (Breed and Sarafis, 1979; Breed, 1997; Flaherty, 1987; Flaherty *et al.*, 1983). The animals reside within the arid region of South Australia and individuals used in the present investigation came from the breeding colony maintained within the Division of Animal Services at The University of Adelaide.

Isolation of the VPs from the Plains Rat Spermatozoa

Spermatozoa were obtained from the caudae epididymides of nine adult males for isolation and extraction of the proteins from the VPs. Because there are between $500x10^6$ and $800x10^6$ sperm stored in the caudae epididymides of an adult plains rat (Breed, 1982, 1986; Pierce and Breed, 1989) this resulted in $5000x10^6$ for extraction. The sperm is sonicated on ice in 20mM Tris-HCl 0.9% NaCl, pH 7.4 (TBS), to break the heads from the tails. The sonicated sperm suspension was then washed several times by low-speed centrifugation and the final pellet resuspended in 80% sucrose, TBS, and centrifuged at 280 000xg for 1h in a 60 Ti angle rotor (Beckman, Missassauga, ON, Canada). The oblong sperm head pellet on the centrifugal side of the tube containing mostly heads was resuspended in TBS and checked for sperm head purity by phase contrast microscopy. If necessary, the ultracentrifugation step was repeated until the fraction contained >99% sperm heads.

Isolated sperm heads were exposed to two successive extraction steps consisting of incubations in 0.2% Triton-X-100 and 1 M NaCl for 1h, each step was followed by a TBS wash. The final pellet was then resuspended in 1 M NaOH for 10 min followed by passing the suspension through a 20-gauge needle several times. The resultant shearing force detached the VPs that were subsequently separated from the sperm head by centrifugation at 100,000 x g through a 20/80% sucrose gradient. The VPs, collected from the sucrose interface, were then diluted in TBS, pelleted by centrifugation, and analyzed by SDS-PAGE, electron microscopy, and Western blotting.

SDS-PAGE and Western Blotting

Isolated VPs were solubilized in 2% SDS/5% b-mercaptoethanol and run on a linear gradient (8-18%) polyacrylamide gel according to Laemmli, 1970. Proteins were electrophoretically transferred from the gels to immobilin-P (0.45um pore size; Millipore, Bedford, MA) in a solution of 25mM Tris-Hcl and 192 mM glycine (pH 8.3) using Hoefer transfer apparatus.

Immunoblotting

The reactivity of the anti-laboratory rat perforatorial and anti-bull perinuclear theca antibodies was investigated on the Western blots of the plains rat VPs, using a secondary antibody (alkaline phophatase-conjugated goat anti-rabbit IgG; Sigma, St. Louis, MO) to detect the signal according to the method of McGadey, 1970.

Immunogold Labeling of Thin Sections and Electron Microscopy

For obtaining mature spermatids and cauda spermatozoa for transmission electron microscopy and immunogold labeling, small pieces of tissue or sperm pellets were immersed in 3% paraformaldehyde/0.5% glutaraldehyde in 0.1 M phosphate buffer, pH 7.4. After fixation for several hours, the tissue was smicated, dehydrated, and embedded in Lowicryl. Thick, 0.5 – to 1-μm, sections were cut with an ultramicrotome, and when appropriate regions were obtained, ultrathin sections were cut and stained with uranyl acetate and lead citrate. These were then incubated with one of the several polyclonal antibodies (anti-PERF 15, anti-PERF 34, anti-PERF 57, and anti-whole PERF antibody) raised against laboratory rat perforatorial proteins (Oko and Clermont, 1988; Oko *et al.*, 1990) as well as bull perinuclear theca proteins (anti-whole bull PT) (Oko and Maravei, 1994). An anti-actin monoclonal antibody (anti-C4) kindly donated by Dr. James Lessard was also used (Lessard, 1988).

RESULTS

Isolation of the VPs

The two VPs are a characteristic feature of the sperm head of Australian hydromyine rodents, to which the plains rat belongs (Fig.1), and they have been shown to form during late spermiogenesis. They develop as extensions of the upper concave surface of the sperm head, joined basally, and differ a little in size with the more apical one being slightly larger (Breed and Sarafis, 1979; Flaherty and Breed, 1983) (Fig. 2A to D). The nucleus evidently protrudes into the base of the processes (Fig. 2A) distal to which there are two fingerlike acrosomal extensions (Fig. 2B). These are surrounded by large amounts of cytoskeletal material within the processes, both of which become progressively more bilaterally flattened toward their tips (Fig, 2 C and D). They contain an extension of the postacrosomal dense lamina at the periphery beneath which filamentous actin occurs (Fig.3) (Breed and Leigh, 1991; Flaherty *et al.*, 1983)

Incubation of sonicated cauda epididymal spermatozoa in 1M NaOH followed by the passing of the sperm suspension through a 20-gauge needle confirmed that this treatment resulted in the detaching of the VPs from the rest of the sperm head (Flaherty and Breed, 1983) (Fig. 4). The VPs were subsequently isolated and collected at the 20%/80% sucrose interface. Although some protein may be lost during this isolation procedure, the VPs retained their shape and most of their electron density suggesting much of the proteinaceous material remained.

Identification of Proteins in the VPs

The isolated sample of VPs was then denatured under reducing conditions (b-mercaptoethanol) and run on SDS-PAGE. When stained with either Coomassie Brilliant Blue or silver a major component was found to have a molecular weight of 15 kDa (Fig. 5). A second major band of 34 kDa was seen when the gels were stained with silver; whether this was visible was dependent on the sample load. Because these molecular weights coincided with the most prominent proteins present in the laboratory rat perforatorium, the proteins were transferred to immobilin-P and probed with antibodies raised against laboratory rat PERF 15 and PERF 34. Western blotting revealed clear immunocross-reactivity to laboratory rat anti-PERF 15 and anti-PERF 34 (Fig. 6) and no reactivity to immune serum (anti-1449) raised against the entire bull perinuclear theca.

To determine the distribution and localization of the 15- and 34- kDa proteins within the VPs, immunogold labeling with anti-PERF 15 and anti-PERF 34 was carried out together with another antibody raised against a less prominent perforatorial protein, anti-PERF 57. Labelling of both VPs and the perforatorium of the apical hook took place after incubation with antibodies to the 15-, 34- and 57- kDa proteins (Fig.7, A to D and Fig. 8, A to C). When the sections were labeled using the monoclonal anti-actin antibody (C4), immunogold staining appeared throughout much of the VPs but did not label the perforatorium of the apical hook (Fig. 8, D to F). However, when the sections were incubated with anti-1449 serum raised against the entire bull perinuclear theca, labeling was restricted to the nucleus and/or acrosome in both the AH and VPs (Fig. 9).

FIGURES

FIGURE 1 - Nomarski differential interference micrograph **(A)** and scanning electron micrograph **(B)** of sperm head of the plains rat showing that, in addition to an apical hook (AH), two VPs extend from the upper concave surface; VS, ventral spur. Transmission electron micrograph of section through a-a is shown in Fig. 2C and b-b in Fig. 2D. Bars: A = 3.5 μm; B = 1.0 μm. (Courtesy of Dr. WB Breed)

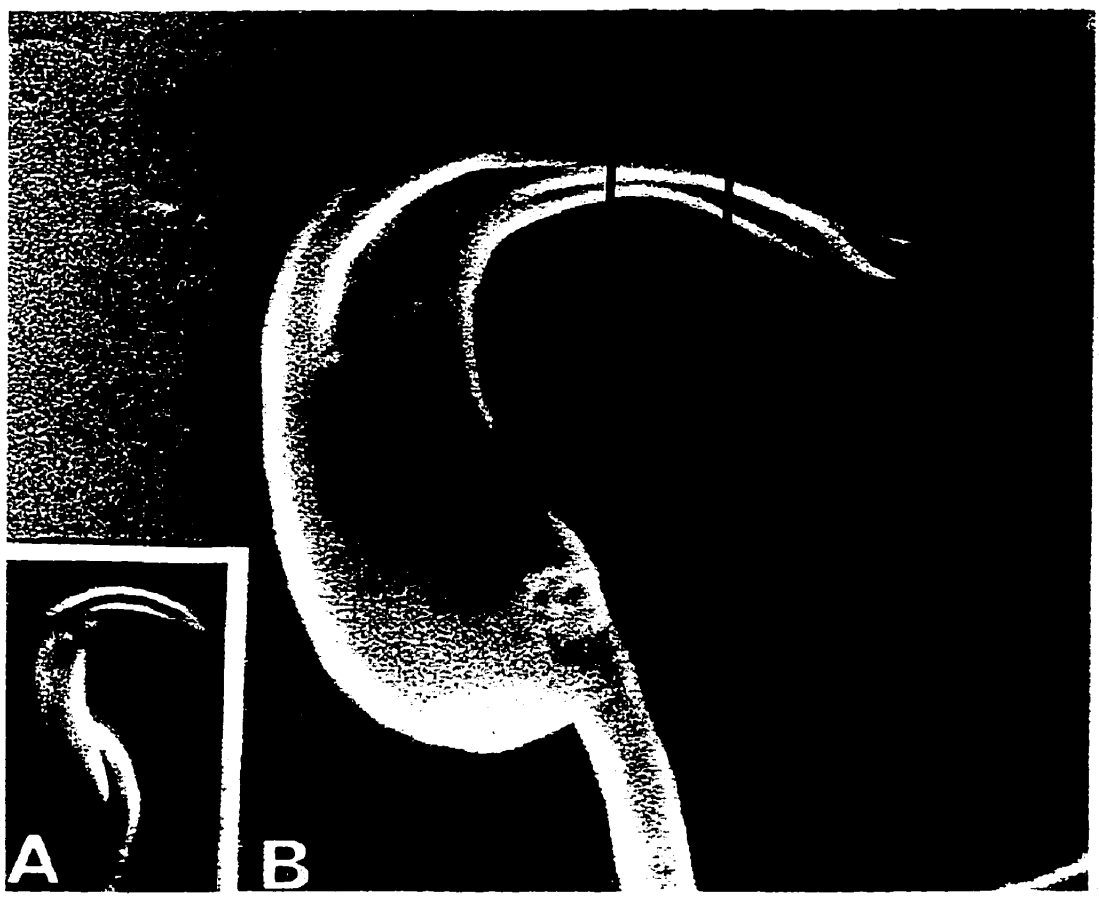
A
B

FIGURE 2 – Transmission electron microscopy of sperm head of plains rat. **(A)** Two large VPs extend from the upper concave surface of sperm head and the nucleus protrudes into the base of these processes. **(B)** Distal to the nucleus a fingerlike acrosomal projection occurs (arrow). This process is, however, very largely composed of electron-dense material that is an extension of the cytoskeleton, and transverse sections show that both processes become progressibely bilaterally flattened distally **(C and D)**. AH, Apical hook; Ac, acrosome; VS, ventral spur. Bars: A = 850 nm, B = 450 nm, C= 100 nm, and D = 140 nm.

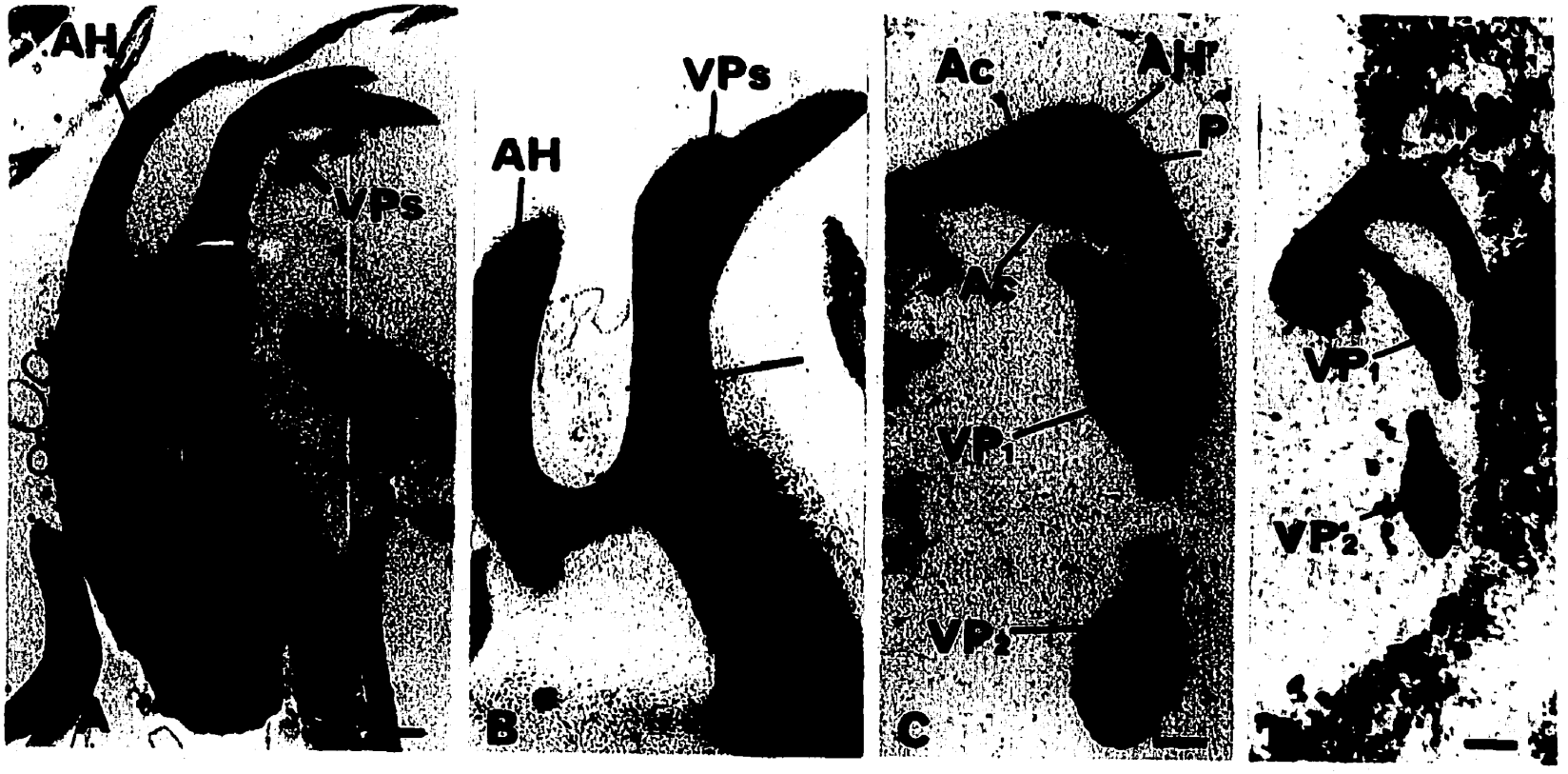
AH
VPs
AH
VPs
Ac
AH
P
As
VP1
VP2
VP1
VP2
B
C

FIGURE 3 – Fluorescent light micrograph of cauda epididymal sperm head of plains rat stained with propidium iodide (a nuclear stain) and Bodipyphallacidin (a stain for filamentous actin). Note the protrusion of the nucleus into the base of the VPs distal to which abundant F-actin occurs, as shown by intensely fluorescent staining with Bodipy-phallacidin (Courtesy of Dr. Breed)

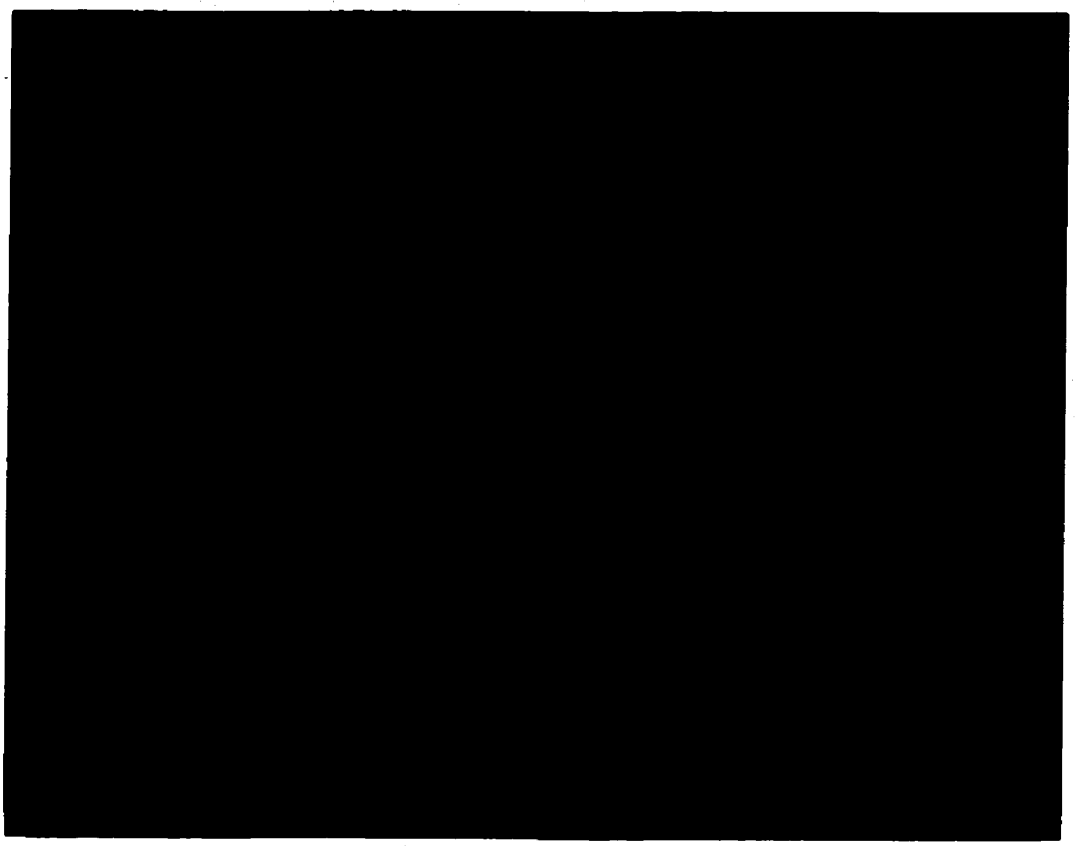

FIGURE 4 – Separation of VPs from isolated sperm heads of plains rats. Intact isolated sperm head showing apical hook (AH) and two VPs **(a)**; X 1250. Sperm head after exposure to 1 M NaOH and shearing through a 20 gauge needle showing that the VPs detach from the head **(b)**; X 1000. Phase contrast survey micrograph of detached VP **(c)**; X 500. Electron micrograph of detached VPs isolated on a discontinuous sucrose gradient **(d)**; note that the VPs retain their density and shape and show their nuclear attachment site (arrow); X 20 000.

Fig. 4

FIGURE 5 – Silver-stained SDS-PAGE of denatured proteins derived from isolated VPs. *Lane S*, molecular mass standards; X 1000. *Lane 1*, polypeptide profile of VPs showing prominent band of 15 kDa and a minor band at 34 kDa.

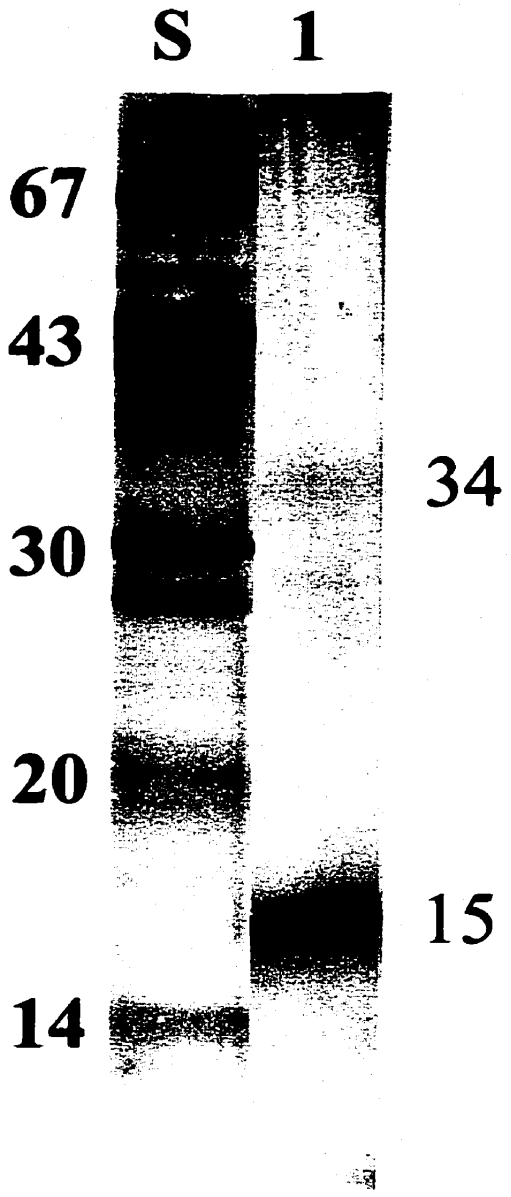
S
1
67
43
34
30
20
15
14

FIGURE 6 – Western blot of VP polypeptides immunostained with anti-perforatorial antibodies. *Lane S*, molecular mass standards, X 1000. *Lane 1*, Coomassie blue-stained VPs polypeptides. *Lane 2*, VP polypeptides immunostained with preimmune serum from rabbit used to obtain antiperforatorial serum. *Lane 3*, VP polypeptides immunostained with antiperforatorial serum affinity purified on isolated 15 kDa perforatorial protein of laboratory rat (anti-PERF 15). Note cross-reactivity with the major 15-kDa protein of VPs. *Lane 4*, VP polypeptides immunostained with affinity purified anti-34 kDa perforatorial serum. The serum cross-reacts with both 34- and 15- kDa proteins of VPs. *Lane 5*, VP polypeptides immunostained with antiserum raised against bull perinuclear theca extract (anti-1449) that normally labels several prominent bull perinuclear theca proteins. No reactivity is evident. The parallel marks in lane 3 and 5 at the 30 kDa level are artifacts of preparation and do not immunostain.

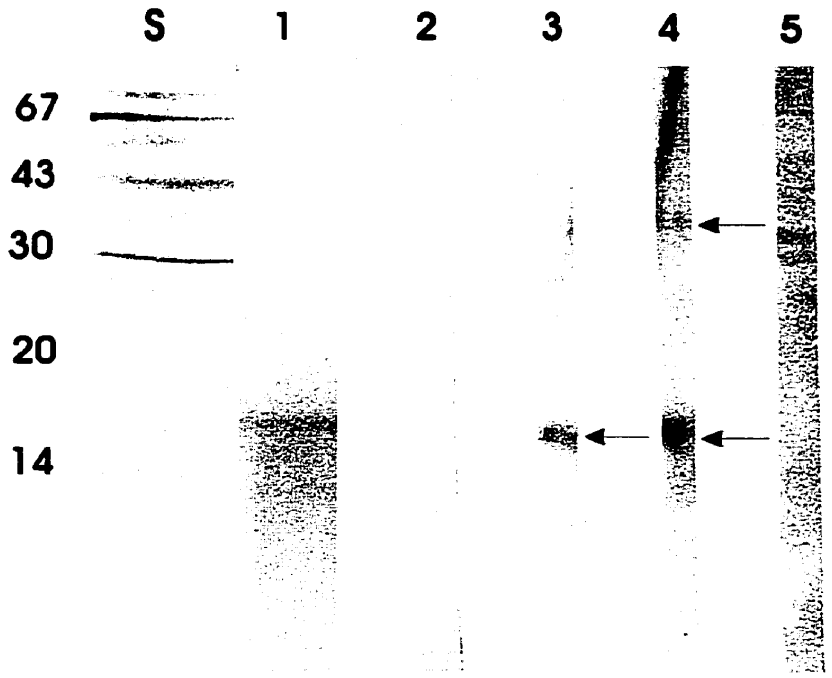
S
1
2
3
4
5
67
43
30
20
14

FIGURE 7 – Transmission electron micrographs of transverse sections through apical hook (AH) and VPs of sperm heads from caudae epididymides after staining with antibody to 15 kDa **(A and B)** and 34 kDa perforatorial proteins **(C and D)**. Note abundance of gold particles over both perforatorium of apical hook and material in both of the VPs (VP1 and VP2). Bars A = 170 nm, B = 170 nm, C = 130 nm, and D = 110 nm.

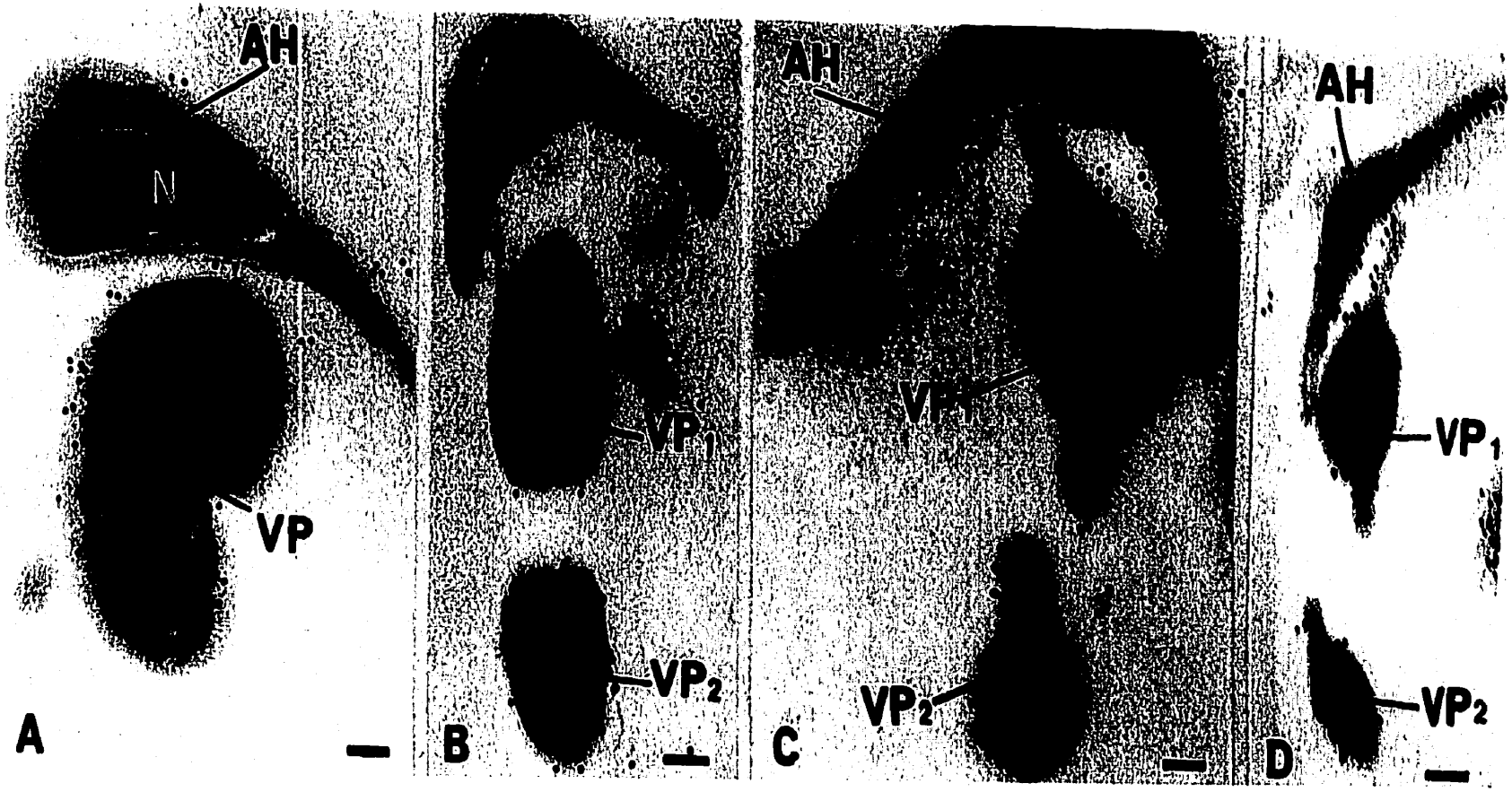
AH
N
VP
A
AH
VP1
VP2
B
AH
VP1
VP2
C
AH
VP1
VP2
D

FIGURE 8 – Transmission electron micrographs of transverse sections through the apical hook (AH) and VPs (VP1 and VP2) of sperm heads from cauda epididymides after staining with antibody to the 57 kDa polypeptide indicating heavy labeling over the material in the VPs as well as the perforatorium in the apical hook but not over the nucleus **(A-C)**, and anti-actin antibody C4 with labeling over the VPs but not over the perforatorium in the apical hook **(D-F)**. Bars A = 170 nm, B =130 nm, C = 170 nm, D = 120 nm, E = 120 nm, and F = 90 nm.


Ac
Ac
A
AH
Ac
VP1
VP2
B
C
AH
VP
D
VP1
VP2
E
VP1
VP2
F

FIGURE 9 - Triton-X-100 and NaCl extracted plains rat sperm head immunogold labeled with anti-1449 immune serum raised against bull perinuclear theca proteins. Labeling is only evident along the periphery of the acrosome (arrows) and nucleus (arrowheads) but absent in the central core of VPs and apical hook (AH). N, Nucleus; VS, ventral spur. Bar = 300 nm.

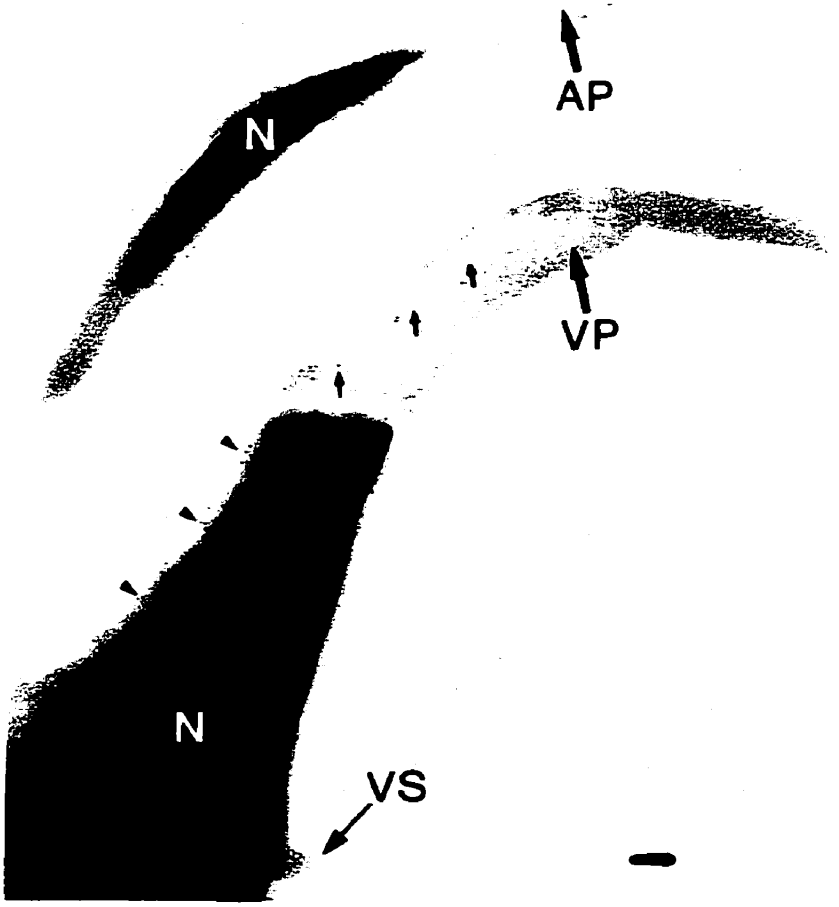
AP
N
VP
N
VS

FIGURE 10 – Summary of distribution of perforatorial proteins (orange) in a diagrammatic sagittal section through the sperm head of the plains rat accompanied by two representative cross-sectional views. Perforatorial proteins are found throughout the dense core of VPs and apical hook (AH). A relatively thin cortex (in yellow border dotted) surrounds the dense core of VPs and is an extension of the postacrosomal dense lamina (PDL). Labels: A, acrosome, stippled regions; N, nucleus; NP, neck/connecting piece. The white dashed line denotes where the caudal-lateral extent of the acrosome would be present on the exterior of the sperm head. Compare with illustrative diagram of laboratory rat spermatozoon (cf. Plate 1; Oko, 1995).

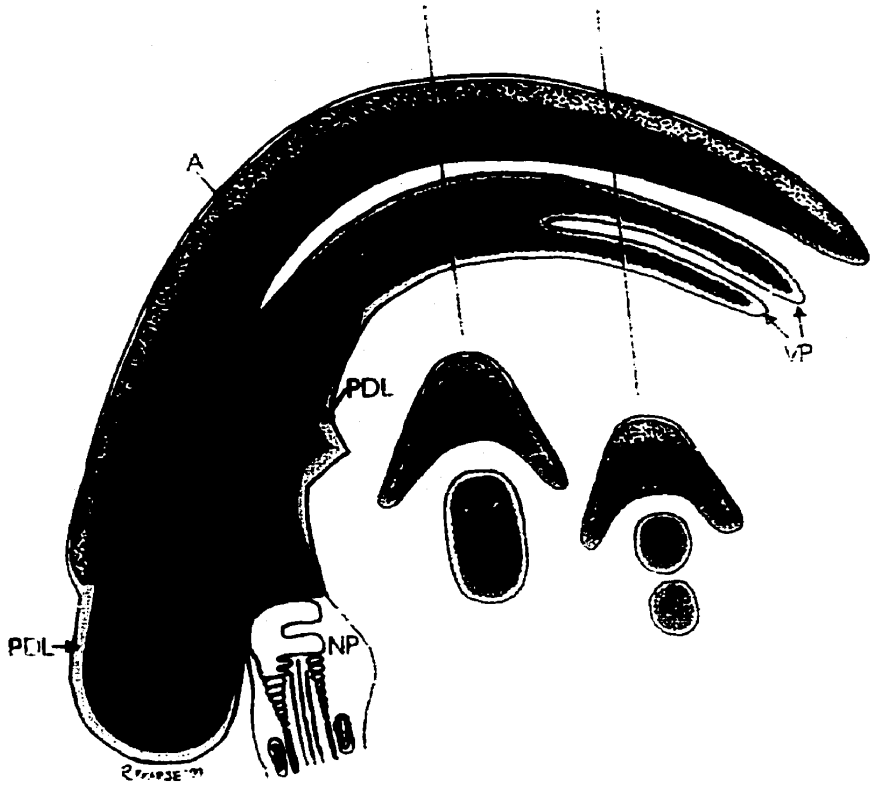
A
VP
PDL
PDL
NP

DISCUSSION

The non-*Rattus* native rodents of Australia are a distinct group of murid rodents that constitute a mixture of about 60 species ranging from small mouselike mammals to others of body mass of about 1 kg (Strahan, 1995). Many other members of this group are also present in New Guinea (Flannery, 1995) but no close relatives have been found in Southeast Asia. Due to their uniqueness and separate evolutionary history from that of other murids, these rodents have been placed within the subfamily, Hydromyinae (Lee *et al.*, 1981; Hand, 1984; Watts and Baverstock, 1995). Studies on spermatozoa of these species have revealed that most members of this group have a very distinctive morphology. Like those of most murid rodents, as exemplified by the laboratory rat and mouse (Friend 1936; Bishoop and Austin, 1957; Bishop and Waltono, 1960; Piko, 1969; Clermont *et al.*, 1955; Lalli and Clermont, 1981), the sperm head is falciform in shape with an apical hook containing the perforatorium (Bishop and Waltono, 1960; Piko, 1969; Clermont *et al.*, 1955; Lalli and Clermont, 1981). For the Hydromyinae, in addition to this structure, two further processes eminate from its upper concave surface just below the AH, termed ventral processes (VPs) [Breed and Sarafis, 1979; Breed, 1983, 1997; Flaherty, 1987; Flaherty and Breed, 1983). Early TEM observations suggested that these structures were an extension of the perforatorium/subacrosomal space (Breed, 1983, 1984; Flaherty and Breed, 1983), however, later work on their morphogenesis indicated that there were two regions of electron density with the peripheral material being an extension of the postacrosomal dense lamina (Flaherty and Breed, 1987; Breed and Leigh, 1991). These VPs stain positively with NBD and Bodipy phalacidin, demonstrating that F-actin is present within them (Breed, 1997; Breed and Leigh, 1991;

Flaherty *et al.*, 1983) (see Fig.3). So far, however, no other proteins have been identified. The presence of other material is evident from the ultrastructural observations of changes that take place during spermiogenesis where, concomitant with their formation, microfilaments of actin can be seen laterally with amorphous material centrally. Furthermore, as maturation proceeds, the VPs change in shape coincident with more electron-dense material accumulating within these structures so that, shortly before spermiation, the actin filaments are no longer visible.

The present study has been conducted to determine what other proteins are present. In the laboratory rat the perforatorium has been shown to contain several proteins that differ from those in the postacrosomal sheath (Oko and Clermont, 1988; Oko *et al.*, 1990) and immunolabeling with antibodies raised against several high molecular weight proteins (34, 43, 57, and 63 kDa) demonstrated their presence throughout the perforatorium and inner layer of the ventral spur, but there was no labeling found within the postacrosomal sheath. Three molecular weight proteins (13, 13.4 and 15 kDa) were found to be restricted to the thicker apical parts of the perforatorium as well as within the inner layer of the ventral spur (Oko *et al.*, 1990)

In the present study antibodies to the 15-kDa (PERF 15) and 34-kDa proteins of the laboratory rat perforatorium cross-reacted strongly with the only two proteins of the same molecular weight from the NaOH extracted and isolated VPs. With the ultra structural observation that the core density of the isolated VPs is preserved, immuno-western blot data shows a similarity in composition between the respective structures with PERF 15 being the dominant shared protein. Subsequent immunostaining of the ultra thin sections of cauda epididymal spermatozoa with antibodies to both the 15-kDa

and 34-kDa proteins confirmed the presence of these proteins in the VPs as well as the 57-kDa protein. These results show that, even though the VPs are surrounded by an extension of the postacrosomal dense lamina, they internally contain material that is composed of at least some of the proteins that are present in the perforatorium, analogous to the ventral spur (VS) of the laboratory rat sperm (Oko *et al.*, 1990). They are not, however, an extension of the VS as scanning and transmission electron microscope of spermatozoa of the plains rat clearly demonstrate its presence separate from the VPs (Breed, 1983, 1984, 1997; Flaherty and Breed, 1983) (see Figs. 1 and 2). Furthermore, our results indicated that the VPs are composed of perforatorial proteins (ie. PERF 15 and 34) that are not found in spatulate spermatozoa of the bull, strongly suggesting that these proteins are specific to members of the murid family of rodents. Figure 10 summarizes our data on the distribution of perforatorial proteins in the plains rat sperm head.

In previous fluorescent light microscopic investigations of the structural organization of the sperm head of the plains rat using NBD phallacidin it was found that the VPs fluoresce brightly, demonstrating the presence of filamentous actin (Breed,1997; Flaherty, 1987; Breed and Leigh, 1991; Flaherty *et al.*, 1983)(see Fig.3). It has been found that spermatozoa of most mammals, including the laboratory rat, contain filamentous actin within the subacrosomal space during maturation, however, F-actin in late spermatids has been shown to depolymerize prior to the release of sperm from the testis (Fouquet *et al.*, 1989; Russell *et al.*, 1986; Vogl *et al.*, 1986; Masri *et al.*, 1987; Halenda *et al.*, 1987). Thus the retention of actin in the mature sperm of the plains rat is unusual. This presence of F-actin was further confirmed by immunogold labeling with a mouse monoclonal anti-actin antibody (Breed and Leigh, 1991) and it has now been

demonstrated with another mouse anti-actin antibody, C4, whereas no staining occurs over the perforatorium as previously found (Oko *et al.*, 1990). Actin's absence in PAGE analysis of the VPs is explainable by its tendency to solubilize in NaOH (R.J.O, personal observation), the solution used in this study to detach the VPs from the sperm head.

What is the function of these VPs and the material within them? Previously, it has been suggested that the material in the perforatorium of the laboratory rat spermatozoon may bind the inner acrosomal membrane to the underlying nuclear envelop and/or maintain the stability of the sperm head membranes during penetration of the egg coats (Oko *et al.*, 1990; Oko, 1995). The cytoskeletal material of the sperm head VPs could not perform such tasks since they do not lie underneath the acrosome, which only occurs as two small separated acrosomal segments surrounded by the cytoskeletal material in the base of the VPs. Furthermore, these VPs could hardly have evolved to maintain the bulk of the sperm head shape as they extend to several micrometers distally from the main body of the sperm head; they are not mechanically viable. In the recent past, there have been several suggested functions of the VPs, however, minimal evidence has been provided for any. It would appear that the processes make contact with the matrix of the zona pellucida during zona binding and penetration studies on oocytes of recently mated animals have clearly shown that these processes become incorporated in the egg cytoplasm at the time of fertilization without undergoing any change in form or apparent structural organization (Breed, 1997; Breed and Leigh, 1991). Thus, as a working hypothesis, it is proposed that the VPs of these Australian hydromyine rodents may form stablilized structures to maintain a region of the cell membrane in which ligands for sperm/zona pellucida binding occur. In vitro and immunogold labeling studies with

antibodies to sperm surface molecules involved in sperm/egg interactions are now required to investigate this possibility.

CONCLUSION

Australian hydromyine rodents have one of the most morphologically complex sperm head structures to have evolved due to the presence of the two ventral processes. In this study, immunolabeling with polyclonal antibodies raised against the entire laboratory rat perforatorium (anti-PERF 15-, 34-, and 57-kDa) as well as a monoclonal antibody (C4) against mouse actin, illustrated the presence of all four proteins within the entire span of the VPs that are surrounded by an extension of the postacrosomal dense lamina. The major protein cross-reacts with anti-PERF 15 antibody. The function of these processes has yet to be determined, but molecules on the plasmalemma surrounding the VPs may participate in sperm/egg binding.

ACKNOWLEDGMENTS

This work was supported by grants from ARC of Australia to W.G.B. and NSERC and MRC of Canada to R.J.O.

CHAPTER 3

COMPOSITION AND DEVELOPMENTAL EXPRESSION OF PROTEINS CONSTITUTING THE SPERM HEAD OF THE PLAINS RAT

ABSTRACT

The Plains rat, *Pseudomys australis*, has a distinctive falciform sperm head structure containing an apical hook and two large ventral processes (VPs). These processes have nuclear material basally, apical to which two finger-like acrosomal projections occur with the rest of their structure composed of a very large extension of the sperm head cytoskeleton. The cytoskeleton of the VPs have been isolated and shown to be composed of perforatorial cross-reacting proteins and F-actin (Breed et al, 2000). Perinuclear theca (PT) proteins on the other hand, characteristic of spatulate sperm head shape, were immunolocalized to regions of the apical hook and VPs adjacent to the acrosomal and nuclear membranes suggesting that perforatorial rather than perinuclear proteins are more fundamental to the falciform sperm head. The major objective of this study was to determine in the Plains rat spermatid the developmental pattern of these two groups of proteins, and possibly gain a better understanding of the cellular events involved in sperm head shaping. Our approach was to first analyze the protein composition of the alkaline extracted Plains rat perforatorial-perinuclear theca (PERF-PT) complex on western blots, using antibodies raised against the laboratory rat PERF and the bull PT as probes, along with a monoclonal antibody directed against F-actin. Once the crossreacting PERF and PT proteins were identified we evaluated and compared the expression and assembly pattern during spermiogenesis in the Plains rat. Immunoprobing of western blot transferred PERF-PT extract indicated that the prominent PERF and PT proteins found in the laboratory rat and bull sperm, respectively, were present in the Plains rat. The predominant polypeptide of the extract was a 15 kDa protein identified as PERF 15 and to a lesser extent: a 34 kDa protein (PERF 34) and PT proteins

PT 15 (SubH2Bv) and PT 60 (Calicin). Immunocytochemistry on testicular sections of the Plains rat testis showed that PT proteins were intimately associated, both temporally and spatially, with acrosome formation from the beginning of spermiogenesis, while PERF proteins began to assemble later in preformed spaces within the subacrosomal and postacrosomal region of elongating spermatids. Although PERF proteins are major components of the apical hook and VPs of murid sperm they do not appear to be determinants of falciform sperm head shape.

INTRODUCTION

Sperm head structure and shape vary markedly among eutherain mammals. There exist two general types of sperm head conformations: (1) a spatulate or paddle-shape typical of bull and human, and (2) a falciform or hook-shape typical of the laboratory rat and mouse (FIG 1) (Fawcett, 1975; Reviewed by Oko, 1995 and Breed, 1997). These two sperm head types have major differences in the extent of development of the cytoskeleton with the falciform shaped sperm having much greater development than spatulate sperm (Lalli and Clermont, 1981). The question posed in this investigation is : does this variation in cytoskeletal material in these two sperm head shapes vary in its protein composition and development.

The sperm head cytoskeleton, or perinuclear theca (PT), is composed of two structurally continuous regions: (1) the subacrosomal layer (SL) which is sandwiched between the inner acrosomal membrane and outer nuclear membrane and which extends apical to the nucleus, as a perforatorium, in falciform-shaped sperm heads, and (2) the postacrosomal sheath (PS) which extends from the posterior end of the acrosomal cap to the implantation fossa and lies between the sperm plasma membrane and the nuclear envelope, see Fig. 1; (Reviewd by Oko *et al.*, 1995). Differences as well as similarities have been shown in PT protein composition of the spatulate sperm head of the bull and of the falciform sperm head of the rat (Oko, 1995; Aul and Oko, 2001; Oko *et al.*, 2001). Similar polypeptide profiles were obtained from the alkaline extracted PT of the bull and lab rat and lab mouse sperm heads, however, in the case of the lab rat and mouse, a 15 kDa polypeptide, identified as PERF 15 (Oko and Morales, 1994; Oko et al, 1997) predominates. The bull PT extract is composed of six major polypeptides, two of which

have been sequenced: a 15 kDa protein termed SubH2Bv or PT15 (Oko and Maravei, 1994; Aul and Oko, 2001) and a 60 kDa protein termed PT 60 or Calicin (Oko and Maravei, 1994; Von Bulow, 1995). These two proteins are also present in the lab rat and mouse PT but in their sperm, unlike that of the bull, they are dominated by PERF 15 (Oko, 1995; Oko *et al.*, 1997; Aul and Oko, 2001). Since both PT 15 and PERF 15 are subacrosomal constituents and both are present in the lab rat sperm head, the distribution of these two proteins within the lab rat sperm perforatorium is of particular interest.

Although both bull and lab rat sperm have common PT proteins, with additional PERF proteins found in the falciform sperm of the lab rat, a distribution and developmental comparison of these two groups of proteins within the sperm head cytoskeleton of a murid rodent has never been carried out. Such a comparison could highlight the differences in composition and perhaps give insight into the significance of the differences in shape that occurs. For this purpose we selected sperm from an Australian murid, *Pseudomys australis*, where there is greater development of sperm head cytoskeleton than any other group of mammals.

The Plains rat, *Pseudomys australis*, is an Australian rodent that has a highly complex sperm head structure in which there is, in addition to an apical hook (AH), similar to the lab rat (Lalli and Clermont, 1981), two elaborate processes, known as ventral processes (VPs), that extend from the upper concave surface of the sperm head (Fig. 1b) (Breed, 1983; Flaherty and Breed, 1987). Our recent study showed these isolated VPs to be perforatorial –like appendages with a similar polypeptide composition to the isolated perforatorium or AH of the lab rat and mouse (Breed *et al.*, 2000). In these processes, the most abundant polypeptide was found to be PERF 15 but immunogold

labeling with anti-PT serum (raised against the extracted bull PT) showed PT proteins occurred in marginal regions of the VPs as well as the AH.

Therefore, in this study we compare the distribution of both the PT and PERF proteins throughout the sperm head cytoskeleton of the Plains rat. The first objective of our investigation was to analyze the protein composition of the entire extracted Plains rat perforatorial-perinuclear theca (PERF-PT) complex and segregate these proteins, by immunoblotting, into respective groups. Both general and specific antibodies against the bull PT and the rat perforatorium were used. Subsequently these antibodies were utilized to compare the distribution and developmental expression of the corresponding proteins in spermiogenesis of the Plains rat. This study shows distinct differences in the temporal and spatial distribution of PT versus PERF proteins during spermiogenesis; this may be related to the final sperm head shape that results.

MATERIALS AND METHODS

Adult male Plains rat, *Pseudomys australis*, was used in this study which came from a breeding colony maintained by colleagues at the Department of Anatomical Sciences, University of Adelaide, Australia.

Separation of Sperm Heads and Tails

Spermatozoa were obtained from the cauda epididymides of nine Plains rat adults. These epididymides were separated from the testes, minced with razor blades and suspended into 20 mM phosphate-buffered saline (PBS), with pH 7.4 at 4°C. This suspension was stirred and filtered through 150 um Nitex netting (Thompson, Montreal, Quebec). The resulting sperm filtrate was centrifuged at 400 X *g* for 10 min, 4°C. The sperm pellet was washed twice with PBS, containing 0.2 mM phenyl methylsulphonyl fluoride (PMSF) and after the last centrifugation, resuspended in 5ml aliquots of PBS. The sperm suspensions were then sonicated on ice with a Bronwill Biosonik IV, VWR sonicator (Scientific, San Francisco, CA) at 50 amps output for 15-s bursts until >99% decapitations had resulted as verified by phase-contrast microscopy. After centrifugation at 400 X g for 10 min, the head-tail pellet of each aliquot was suspended into 30 mL of an 80% sucrose solution and ultra-centrifuged at 50,000 RPM for 1 hr in a 60 Ti angle rotor (Beckman, Mississauga, ON) to separate the heads from tails. The sperm head pellet on the centrifugal side of the ultracentrifuge tube was transferred to a new tube, resuspended in 20 mM PBS and further washed by high speed centrifugation. The technique was adapted from Oko and Maravei (1994).

Extraction of the Plains Rat Perinuclear Theca

To obtain the perinuclear theca proteins, the isolated sperm head fraction was exposed to three successive extraction steps consisting of incubations in 0.2% Triton X-100, 1M NaCl and 100mM NaOH at 4°C. In the first two extractions the sperm head fraction was suspended for 1 hr with shaking while the NaOH extraction required an overnight incubation with agitation. After each extraction, the supernatent was recovered by centrifugation at 1000 X *g* for 15 min at 4°C and the resulting pellet rewashed in 25 mM Tris-Buffered Saline (TBS), pH 7.4 at 4°C before being subjected to the next extraction (Oko and Maravei, 1994). The NaOH supernatant, containing the bulk of the PT proteins, was dialyzed overnight against three changes of distilled water, followed by lyophilization for future analysis.

Antibody Preparation

Anti-sera was raised in rabbits against the lyophilized NaOH bull extract (anti-1449); (Oko and Maravei, 1994) and against the isolated laboratory rat perforatorium (anti-4442); (Oko and Clermont, 1988). The antisera were used directly for immunoblotting and immunocytochemistry or indirectly for the affinity purification of specific antibodies against PT and PERF proteins isolated on westerns. Anti-1449 was used to affinity purify antibodies against western blot isolated PT15 and PT60 while anti-4442 was used to affinity purify antibodies against isolated rat PERF 15 and PERF 34 according to Oko and Morales (1994) and Oko and Maravei (1994). Briefly, the desired polypeptide band detected by Ponceau rouge was cut out from five preparative western

blots, cut into 3 mm^2 pieces, and inserted into 10 cc syringes to form the affinity purification column. The columns were incubated with 5 mL of TBS containing 10% goat serum for blocking, followed by a 1 hr incubation in the appropriate 1:100 antisera diluted in TBS, pH 8.0, with continual shaking. After adsorption, the columns were thoroughly washed in 5 x 5 min changes of TBS + 0.5 % Tween, with continual shaking, to remove nonadsorbed or nonspecific antibodies. The specific antibodies were eluted from the column after incubation in 5 mls of 0.2 M glycine-HCl, pH 2.8 for 3 min. and immediately neutralized in an equal volume of double strength TBS, pH 12.5. The neutralized elute was concentrated to approximately 2-3 mL with a Centriprep 30 concentrator (Amicon, Beverly, MA) and utilized directly for immunoblotting, followed by further concentration to about 200 uL with a Centricon 10 microconcentrator (Amicon, Beverly, MA) and utilized directly for immunocytochemistry. The above procedure was adapted from Talian *et al.* (1983). The antiactin mouse monoclonal antibody, anti-C4, was kindly obtained from Dr. James L. Lessard.

SDS-PAGE and Western Blotting

The lyophilized PT extracts were solubilized in 2% SDS/5% B-mercaptoethanol for 10 min at 100°C and run on a 15% discontinuous linear gradient polyacrylamide gel according to Laemmli (1970). Approximately 5 μg of protein was loaded in each gel lane, and, in the case of preparative gels, approximately 50 μg of protein was loaded per gel. The apparent molecular weights of the proteins were determined by comparison to

the low molecular weight standards (Pharmacia Electrophoresis Calibration Kit, Piscataway, New York).

Gel immobilized proteins were western blotted onto polyvinylidene difluoride (PVDF) (0.14μm pore size, Millipore, Mississauga, ON) in 25 mM Tris-base, 192mM Glycine, 0.04% SDS buffer in Hoefer Transphor Apparatus (Hoefer Scientific Instruments, San Francisco, CA) or a Mini Trans-Blot Electrophoretic Transfer Cell (Bio-Rad, Hercules, CA) according to procedure of Towbin (1979). Electrophoretic transfer was carried out at 250 mM for 60 min or 100 mA for 1-2 hours, respectively. After transfer, the PVDF blots were washed in TBS (10 mM Tris-HCl, 0.9% NaCl, and 0.5% Tween-20) and then selected strips stained with Coomassie Brilliant Blue Dye or Ponceau Rouge to examine efficiency of transfer.

Immunoblotting

Strips from the preparative western blot were washed in three 5-min changes of 10mM TBS (Tris-HCl, 0.9%NaCl, pH 7.4) saturated with 10% normal goat serum (NGS) in 10mM TBS for approximately 30 min. and incubated with primary antibodies for 2 hours at room temperature, or overnight at 4°C. Anti-sera was diluted 1/100 in TBS, while affinity purified antibodies were used undiluted. The strips were then rinsed 5 x 5 min in TBS + 0.1% Tween-20 and again saturated with 10% NGS for 15 min before incubation with secondary antibody (alkaline phosphatase-conjugated F(ab)2 goat anti-rabbit immunoglobulin G [IgG] (Boehringer Mannheim, Germany), at a concentration of 1:1000 in TBS, for 1 hr. After several washes in TBS + 0.1% Tween, enzymatic colour

detection was performed according to McGadey (1970) in 50 mM Na-glycinate, pH 9.6 containing 0.1 mg/mL of 4-nitroblue tetrazolium chloride, 0.05 mg/mL of 5-bromo-4-chloro-3-indolyl phosphate and 1M $MgCl_2$.

Tissue Preparation and Immunogold Labeling of Ultrathin Sections

Animals were anaesthetized and testis and epididymides perfused with fixative via the thoracic aorta before small 1 mm^2 pieces of testis were cut and immersed for several hours in the same fixative (3% glutaraldehyde/3% paraformaldehyde made up in 0.1 M phophate buffer, pH 7.35, containing 2.5% polyvinylpyrrolidone (PVP). After washing and dehydration the tissue was embedded in LR White resin (hard grade, London Resin Co, UK) in gelatin capsules and polymerized at 60°C for 24 hrs. Ultrathin sections were cut and collected on formvar coated nickel grids. The sections were then blocked with 10% NGS for 30 min. and incubated in primary antibodies for 2 hrs. Anti-sera were diluted 1/100 in TBS before use while affinity purified antibodies were used straight. After incubation the sections were washed 4 X 5 min each in TBS containing 0.1% Tween-20, followed by another saturation (or blocking) with 10% NGS for 15 min. before secondary antibody (10nm colloidal gold-conjugated goat anti-rabbit IgG, Sollinger Inc. Montreal) with an incubation period of 1 hr. The tissue sections were then washed 4 X 5 min. in TBS + 0.1% Tween-20, and 2 X 2 min. washes in dH2O before counterstaining with uranyl acetate for 2 min and lead citrate for 30 s. The sections were examined under a Hitachi 7000 Transmission Electron Microscope.

Tissue Preparation and Immunoperoxidase Staining of Paraffin Sections

Testis were perfused in Bouin's fixative and embedded in paraffin. Five μm sections were cut, deparaffinized in xylene, followed by hydration in a graded series of decreasing ethanol concentrations. During this hydration period, the sections were treated for 5 min in 70% ethanol containing 0.15% hydrogen peroxide and another 70% ethanol solution containing 1% Lithium carbonate. After hydration the sections were incubated for 5 min in 300mM glycine prior to immunoperoxidase staining by one of two methods. Tissue preparation was identical to that already described by Oko *et al.* (1996).

The two step indirect method followed an identical protocol already described for immunogold labeling except the secondary antibody used was conjugated to peroxidase (Boehringer Mannheim, Germany) for enzymatic colour development. The three step ABC method for intensifying the reaction followed the procedure of Vector laboratories (Burlingham, CA) using the Vectastain Elite ABC Kit. Briefly, paraffin sections were blocked with avidin block for 15 min, washed 5 X 5 min in TBS, blocked with biotin block for 15 min, washed 5 X 5 min in TBS, blocked with 10% GS for 15 min, incubated with appropriate primary antibody for 2 hrs at 24°C or overnight at 4°C and washed 5 x 5 min in TBS. Sections were then blocked with 10% GS for 15 min, incubated with biotinylated goat anti-rabbit secondary antibody for 30min, washed 5 x 5 min in TBS-Tween and incubated with ABC Reagent mix (1:100 dilution) for 30 min. After 5 x 5 min washes in TBS-Tween, the peroxidase substrate colour reaction was developed in TBS, pH 7.6, containing 0.03% hydrogen peroxide, 0.05% diaminobenzidene tetrahydrochloride (DAB) and 0.1 M imidizole. After washing in dH2O, the sections

were counterstained with 0.1% methylene blue, dehydrated in 50%, 70%, 95%, and 100% gradient ethanol solutions, immersed in Xylene and mounted in permount.

Staging of the Plains rat Seminiferous Tubules: Fourteen stages (I-XIV)

The classification scheme developed by Leblond and Clermont (1952) on the lab rat was used in this study to stage the seminiferous tubules of the Plains rat.

RESULTS

Extraction of the Plains Rat PT

The plains rat sperm, retrieved from eighteen epididymides, were sonicated until >99% decapitation was achieved (Fig. 2a). The sperm heads were then separated from the tails on a 80% sucrose gradient and subjected to a three step PT extraction protocol (see Methods and Materials). Sequential 0.2 Triton X-100 and 1 M NaCl extractions (Steps 1 and 2 of isolation protocol) removed the sperm head membranes and acrosome leaving an insoluble perinuclear theca that included part of apical hook and VPs together with the condensed nucleus (Fig. 2b). The PT was subsequently solubilized in the final NaOH extraction step leaving behind only the condensed nucleus (Fig. 2c). The supernatent of this alkaline extraction step was then dialyzed and lyophilized for compositional analysis of the PT structure.

Compositional Analysis of the Plains rat PT

SDS-PAGE analysis of the lyophilized NaOH PT extract of the Plains rat revealed a polypeptide profile (Fig. 3, Lane 1) similar to the NaOH PT extract of the laboratory rat (Fig. 3, Lane 2). A 15-kDa polypeptide band predominated in both cases and co-migrating bands of 43- and 60-kDa, amongst others ranging from 24- to 36- kDa, were found to occur.

Strips of the preparative western blot of the Plains rat PT proteins were probed with the following rat PERF and bull PT antibodies: anti-whole PERF (4442), affinity purified anti-PERF 15 and anti-PERF 34, anti-whole bull PT (1449), anti PT-15 (SubH2Bv) and anti-PT 60 (Calicin) (Fig. 4). A pan monoclonal anti-actin antibody (C4)

was used to detect the presence of actin. All of the affinity purified and general antibodies listed above were found to be cross-reactive with Plains rat PT proteins (Fig. 4). Three of the affinity purified antibodies reacted mono-specifically, ie.anti-PERF15, anti-PT15/SubH2Bv, and anti-PT60 (Calicin). Anti-actin antibody stained the 43 kDa band most strongly (Fig. 4, lane 10).

EM Immunogold labeling of Plains rat Cauda Epididymal Sperm

Four antibodies were chosen for immunogold labeling of the Plains rat sperm head. These were the two anti-whole PERF and PT sera and the affinity purified anti-PERF 15 and anti-PT 15 antibodies.

At the ultrastructural level, immunogold labeling of plains rat sperm sections, taken from at least three different blocks of fixed epididymal tissue, illustrated distinctive spatial differences in the distribution of PERF and PT proteins. Immunogold labeling with anti-PERF (4442) and anti-PERF15 as expected labeled the bulk of material making up the perforatorial appendages (AH and VPs) (Fig. 5a). In contrast, anti-PT (1449) and anti-PT15 (SubH2Bv) labeling in the subacrosomal region was restricted to a marginal area on the periphery of the acrosome and nucleus (Fig. 5b). Interestingly, the periphery of the separated acrosomal head cap segments of both AP and VP were outlined by gold labeling. Labeling with the monoclonal anti-actin antibody (C4) was present in the VPs but not APs of the mature Plains rat spermatozoa (Fig 5c, Breed *et al.*, 2000).

Immunoperoxidase Staining of Plains rat testicular sections

Before analyzing the Plains rat testicular paraffin sections, which were taken from at least three different blocks of fixed testicular tissue, lab rat and bull testicular sections were studied using anti-whole PERF and anti-whole PT antibodies, respectively, in order to provide a comparison and control when determining the developmental pattern associated with each group of proteins in the Plains rat. In lab rat sections immunostained with anti-PERF antibody pachytene spermatocytes were weakly reactive when compared to spermatids. However the most intense reaction was over the elongating spermatid population (Fig. 6a). On the other hand, immunoperoxidase labeling of bull testicular sections using anti-whole PT revealed an entirely different pattern that was restricted to the spermatid population. A reaction was first evident surrounding the acrosomic vesicle of early-round spermatids (Fig. 6b – stage III) in the Golgi phase, it remained closely associated with the crescent-shaped acrosome during the cap phase (stage VII) and finally followed the contour of the acrosome in the elongated spermatids (X) (Fig. 6b).

As was the case in the lab rat, anti-PERF (4442) and anti-PERF 15 antibodies reacted preferentially with the elongating spermatids of the Plains rat (Fig. 7a, b). However, in contrast to the lab rat where the labeling was most intense in the elongating spermatid cytoplasm of steps 9 to 14 (stages IX-XIV), the labeling in the Plains rat was most intense in the cytoplasm of late elongating spermatids from steps 16 to 18 (stages II to VI), reminiscent of the results obtained by Oko *et al.* (1997) in the mouse. More importantly, perforatorial immunoreactivity first became associated with the acrosomal / subacrosomal region of step 8 late round spermatids (stage VIII, Fig. 7b) and then

intensified over the head region of early elongating spermatids in steps 9 to 14 (see stage XI and XII in Fig. 7a)

Anti-PT reactivity, on the other hand, was associated with the acrosome from the beginning of its morphogenesis (step 1) to its end (step VIII, Fig. 8) reminiscent of the results obtained in the bull. Thereafter, the immunoreactivity conformed to the changing shape of the acrosome as the spermatid head elongated.

Ultrastructural development of the apical hook and ventral processes

It was evident by Step 15 of spermiogenesis (according to lab rat staging) that the shape of the AH and VPs had already formed before the condensation of the cytosolic core contained within. Only minor peripheral condensation of presumably perforatorial proteins occurred (Fig. 9 a). By step 18 of spermiogenesis condensation of the cytosolic cores became more evident (Fig. 9b; arrows) and by step 19, spermatid condensation of these spaces was complete (Fig 9 c). Note that this development is parallel to that of the laboratory rat as shown by Oko and Clermont (1991).

Immunogold labeling of Plains rat Testicular sections

Anti-whole PT and anti-PT 15 (SubH2Bv) antibodies were associated with the acrosome in early spermatid development (Step 5, Fig. 10 a). Interestingly, the assembly of PT proteins within the Plains rat ends at step 7 when the acrosome has fully formed and shape changes begin. Labeling continues to underlay the acrosome in the subacrosomal layer, surrounds the separated head segments in the SL and VPs as well as lines the outer periacrosomal membrane in the equatorial region (Step 17, Fig. 10 a & b).

In the final step of spermiogenesis, step 19, when the perforatorial proteins condense, the labeling remains restricted to the acrosomal and nuclear membranes in the AH, in contrast to its absence in the VPs (Fig. 10 c).

The pattern of immunogold labeling on testicular sections reacted with anti-whole PERF and PERF15 antibodies was identical, as previously described in the lab rat (Oko *et al.*, 1990; Oko and Clermont, 1991). The PERF proteins were labeled in both the cytoplasm and nucleus of pachytene spermatids (not shown). Before the descent of the manchette (M), consequent formation of the postacrosomal sheath and displacement of the immunogold labeled cytoplasmic lobe, the "track" of the manchette between the displaced cytoplasm and forming subacrosomal layer (indicated as spaces - S) shows labeling (Fig 11 a&b). A gradual increase in labeling intensity was seen in the SL of the AH and the core of the VPs in steps 17 and 18 (not shown), before full perforatorial condensation, and hence intense labeling of the VPs and AH cores, in Step 19 spermatids (refer to Fig. 11 c). Note the labeling of the nucleus (N) and the cytoplasmic lobe is intense, while the Sertoli Cell cytoplasm does not label.

FIGURES

FIGURE 1 – (a) Diagrammatical representation of a mid-saggital section through the *falciform* shaped head of a rat spermatozoon. The region delineated in red, between the acrosomal cap (A) and the nucleus (N) is the subacrosomal layer/perforatorium. The region delineated in yellow is the postacrosomal sheath **(b)** Diagrammatical representation of the Plains rat sperm head with an apical hook/process (AH/AP) and two ventral processes (VPs) extending from its upper concave surface. A, acrosome; N, nucleus; PDL, postacrosomal dense lamina or postacrosomal sheath. **(c)** Diagrammatical representation of a mid-saggital section through the *spatulate* shaped bull spermatozoon.

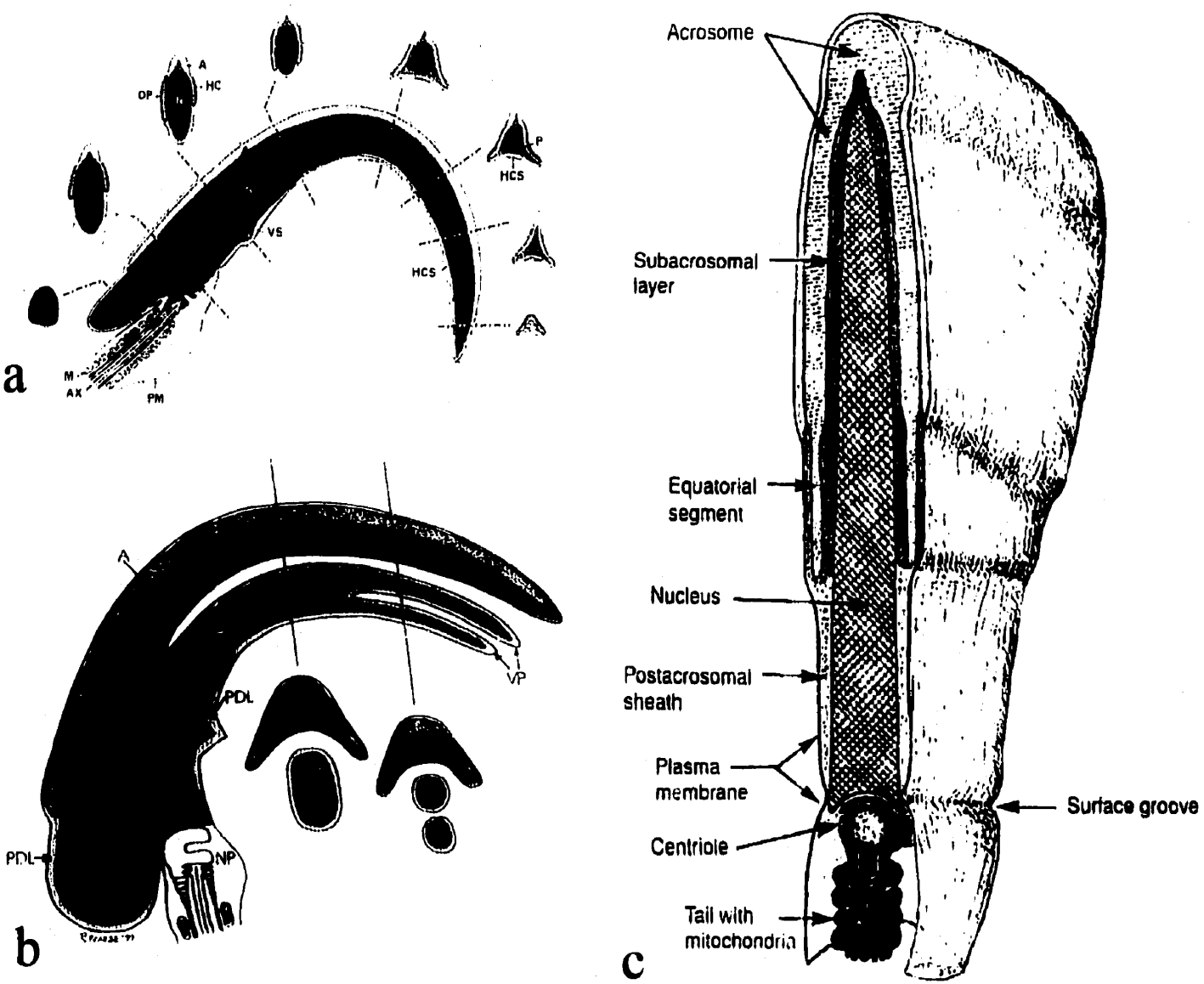
a
A
OP
HC
P
HCS
VS
HCS
M
AX
PM
b
A
VP
PDL
PDL
NP
c
Acrosome
Subacrosomal layer
Equatorial segment
Nucleus
Postacrosomal sheath
Plasma membrane
Centriole
Tail with mitochondria
Surface groove

FIGURE 2 – Micrographs showing steps involved in the extraction of the Plains rat Perinuclear theca. **(a)** Phase contrast microscopy of sperm heads separated from the tails. **(b)** Electron Micrograph typical of the isolated sperm head after sequential KCl and Triton-X-100 extractions. Note the retention of the PT around and rostral to the nucleus. VPs, ventral processes; AP, apical process/hook; N, nucleus; Bar, 0.2 μm. **(c)** Electron micrograph of sperm nucleus after extraction of the PT with 100 mM NaOH. Note that no remnant of PT remains. Bar = 0.2 μm.


AH
VP
AH
b
c

FIGURE 3 – Coomassie Brilliant Blue stained 15% linear gradient SDS-PAGE gel of Plains rat, *Lane* 1, and lab rat, *Lane* 2, PT extracts. The molecular weight standards, *S*, are denoted by number x 10^3.

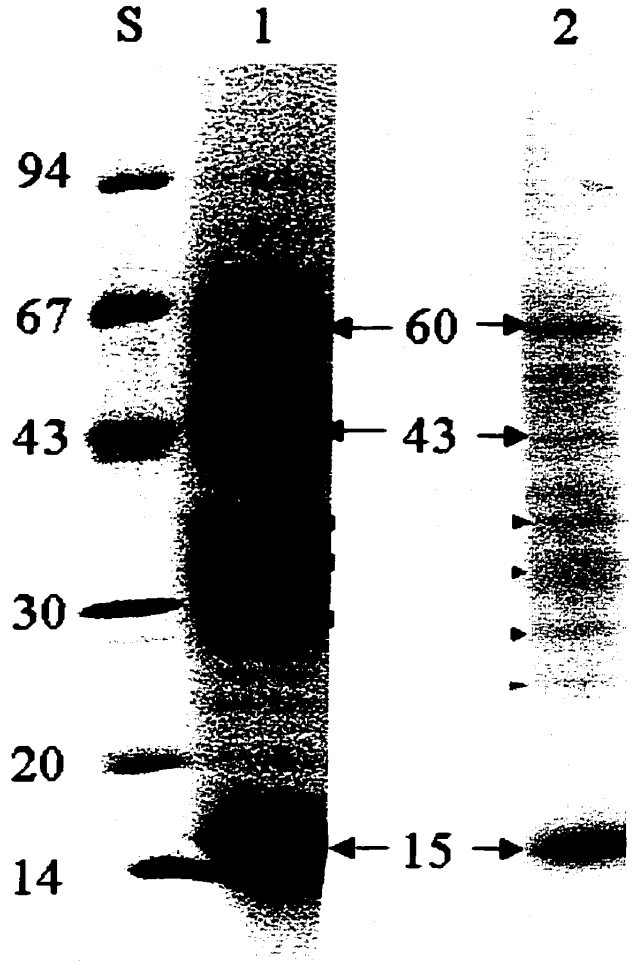
S
1
2
94
67
43
30
20
14
60
43
15

FIGURE 4 – Preparative Western Blot of Plains rat PT extract immunostained with rat PERF and bull PT antibodies. *Lane S*, molecular weight standards X 10^3. *Lane 1*, Coomassie brilliant blue stained Plains rat PT transferred polypeptides. *Lane 2*, rat anti-whole PERF (4442) preimmune serum control. *Lane 3*, PERF (4442) immune serum raised against isolated whole rat perforatorium. *Lane 4*, anti-PERF15 antibody. *Lane 5*, anti-PERF 34 antibody. *Lane 6*, bull anti-whole PT (1449) pre-immune serum control. *Lane 7*, anti-PT (1449) serum against whole bull PT. *Lane 8*, anti-PT 15 (SubH2Bv) antibody. *Lane 9*, anti-PT 60 (Calicin) antibody. *Lane 10*, anti-actin antibody (C4) (Breed et al., 2000).

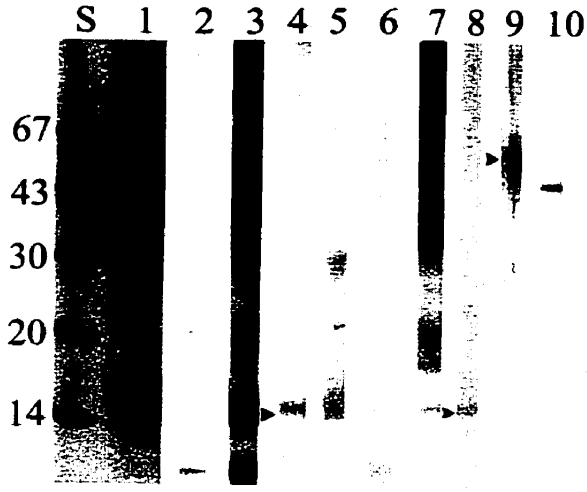
S 1 2 3 4 5 6 7 8 9 10
67
43
30
20
14

FIGURE 5 – Immunogold labeling of Plains rat cauda epididymal sperm sections with anti-PERF and anti-PT antibodies. **(a)** Longitudinal section of demembranated sperm labeled with anti-whole PERF (4442) antibody. The perforatorial material in the AH and VPs is strongly labeled. **(b)** Longitudinal section of demembranated sperm labeled with anti-whole PT (1449). Labeling is restricted to the periphery of the acrosome and nucleus but absent in the central core of the VPs and AH. **(c)** Cross-section labeled with anti-actin antibody (C4) where immunogold labeling is localized to the region of the VP with only a few gold particles found in the AH of the mature spermatozoa (courtesy of Breed et al., 2000). N, nucleus; VP, ventral process; AH, apical hook; SA, separated acrosomal head segments. Bars = 0.2 μm.


AH
VP
SA
AH
VP
SA
N
AH
VP
AH
Ac
VP
C

FIGURE 6 – (a) ABC immunoperoxidase staining of laboratory rat seminiferous tubules paraffin sections using anti-whole PERF (4442) antibody. The immunostaining is most intense over the early elongated spermatid population (stage XII) on the inner most aspect of the tubule. In comparison, in decreasing order, it is also present in round spermatids and mid- to late pachytene spermatocytes. Bar = 10 μm. **(b)** ABC immunoperoxidase staining of bull seminiferous tubules using anti-whole PT (1449) antibody. The reaction product surrounds the acrosomic vesicle (arrow heads) of early-round spermatids (III), remains associated with the acrosome as it spreads and caps the round spermatid nucleus (VII), and continues its acrosome association in elongating spermatids (X). MP, mid-pachytene; RS, round spermatid population; LP, late pachytene spermatocytes; EP, early pachytene spermatocytes.. Bar = 10 μm.

VII

FIGURE 7 – ABC immunoperoxidase staining with anti-PERF antibodies on paraffin sections of the seminiferous tubules representing various stages of the cycle of seminiferous epithelium in the Plains rat. The anti-whole PERF antiserum **(a)** and anti-PERF-15 antibody **(b)** indicated identical patterns of labeling. With both antibodies the immunoreactivity first became evident in mid-pachytene spermatocytes (MP), then becomes more evident in round spermatids (RS), gradually increases in elongating spermatids (ES), becoming most intense in the cytoplasm of late elongating spermatids (see stages IV and V). Perforatorial reactivity associated with the acrosomal / subacrosomal region is first seen in a few round spermatids in stage VIII (arrows) and in the majority of elongating spermatids by stages XI-XII (arrows) Sg., Spermatogonia; ES, elongating sprematids; RB, residual body. Bars = 10 μm.

XII
VI
XII
VI

FIGURE 8 – Immunoperoxidase staining with anti-PT antibodies of seminiferous tubules representing various stages of the cycle of the seminiferous epithelium of Plains rat. **(a)** Shows the extent and pattern of immunoperoxidase staining, using the two-step indirect method, obtained with the anti-whole bull PT antibodies (1449). The reaction is restricted to the spermatid population and is associated with acrosome morphogenesis. Plains rat testicular sections immunostained, using the ABC method, with **(b)** anti-pan bull PT and **(c)** anti-PT15/SubH2Bv antibody. Arrows and arrowheads point to reaction product associated with the acrosome cap and acrosome vesicle, respectively. The specificity of the immunoreaction is identified for both antibodies and comparable to that seen in the bull seminiferous epithelium in Fig. 5a. Bars = 10 μm.


V-VI

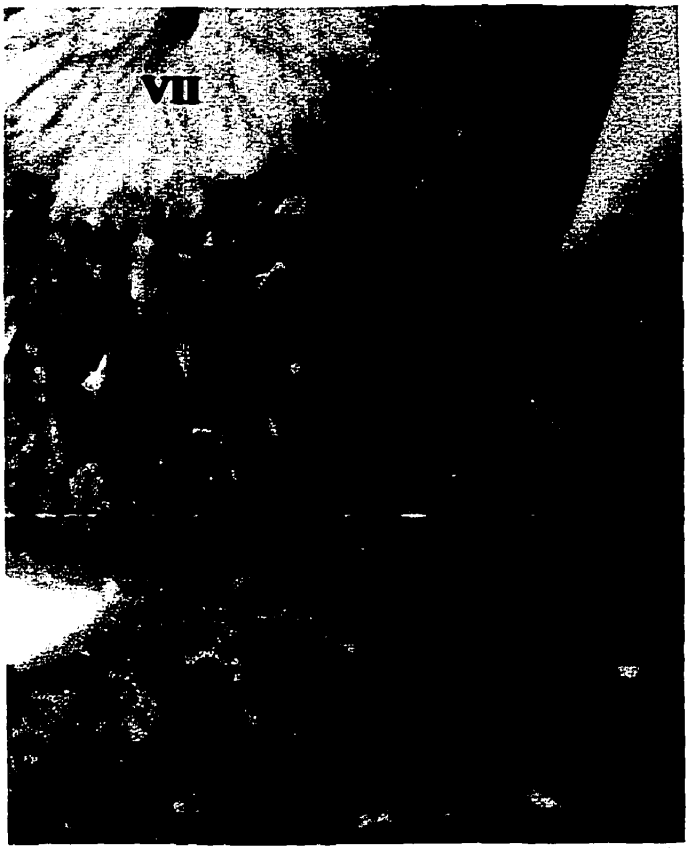
VII

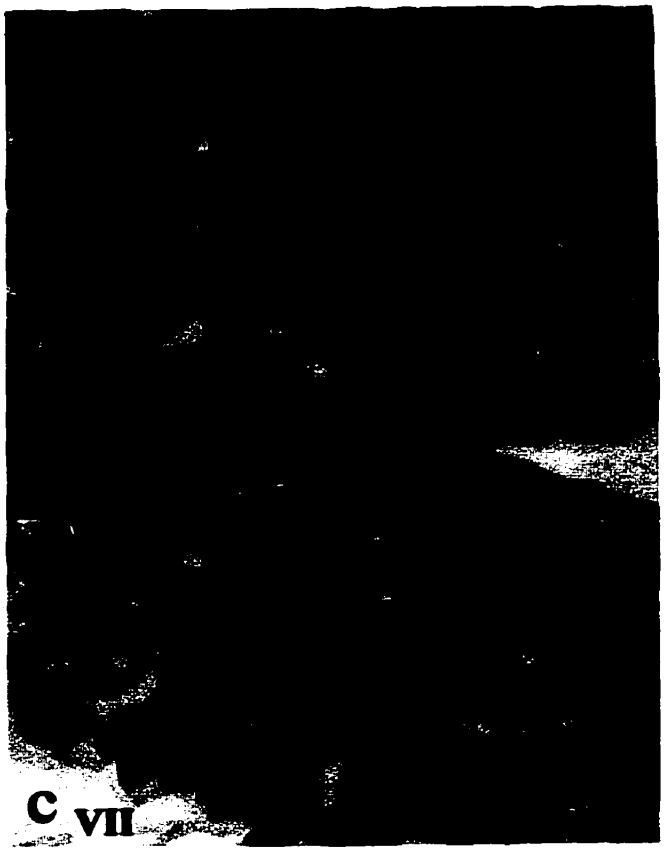
C VII

FIGURE 9 – Transmission Electron Micrograph sections of the Plains Rat (PR) sperm head during steps 15,18 and 19 of spermiogenesis. **(a)** Sagittal section of Plains Rat at step 15 in spermiogensis where the nucleus (N) has already condensed and taken its definitive shape yet the perforatorial cores of both AH and VPs remain uncondensed. Evidence of initial cytoplasmic condensation can be seen at the periphery of the sperm head, in both the AH and VPs, in most cases close to the inner-acrosomal membrane. **(b)** Cross-sections of the Plains rat sperm head at step 18 where there is an increase in cytoplasmic condensation in both the AH and VPs. **(c)** Sections through AH and VPs of step 19 spermatids illustrating the final condensation of perforatorial core (P) condensed within; SA, Separated acrosomal head segments. Bars = 0.2 μm.

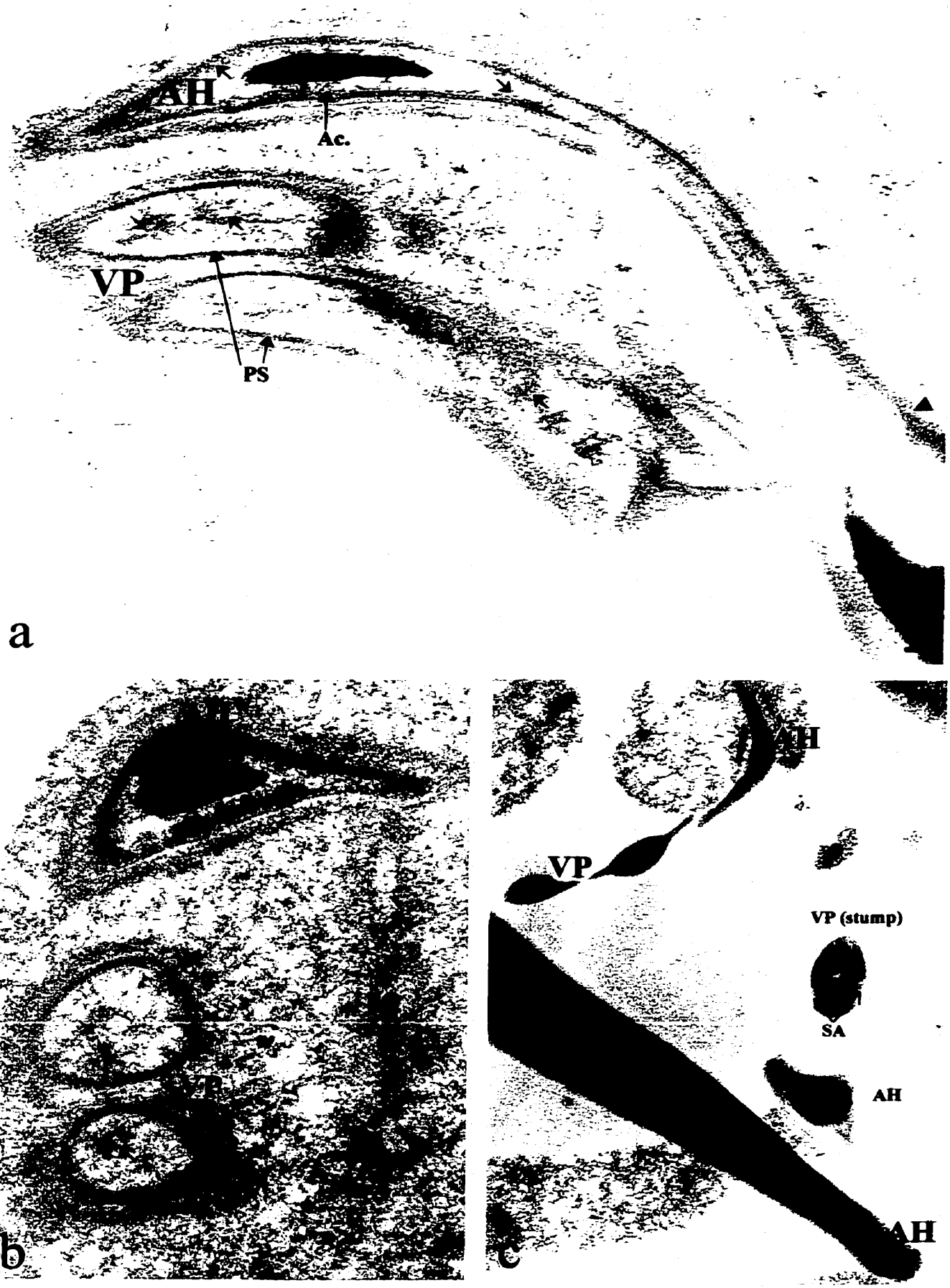
AH
Ac.
VP
PS
a
b
AH
VP
VP (stump)
SA
AH
AH
c

FIGURE 10 – Plains rat testicular sections immunogold labeled with anti-bull PT antibodies all of which displayed identical patterns of labeling. (a) An oblique section of a step 5 round spermatid and an elongating step 17 spermatid labeled with anti-whole bull PT. The former illustrates specificity of labeling to the area underlying the acrosome (arrows) and the latter illustrates labeling also associated with the acrosome of the AH and the outer periacrosomal membrane in the equatorial region (ER) (arrows). (b) Sections labeled with anti-PT15/SubH2Bv antibodies of elongating spermatids when the manchette (M) has just descended and the consequential formation of the postacrosomal sheath (PS) (arrowhead); note the cytosolic spaces forming in the core of the perforatorium are not labeled, in contrast to what happens with anti-PERF antibodies in Fig.11. (c) Cross-section of step 19 spermatids, when the perforatorium has just condensed, labeled with anti-whole PT antibody. Once again, gold particles are restricted and associated with the acrosomal and nuclear membranes in the apical hook (AH) and absent in the VPs. Bars = 0.2 μm.


ER
a
N


S
S
S
b

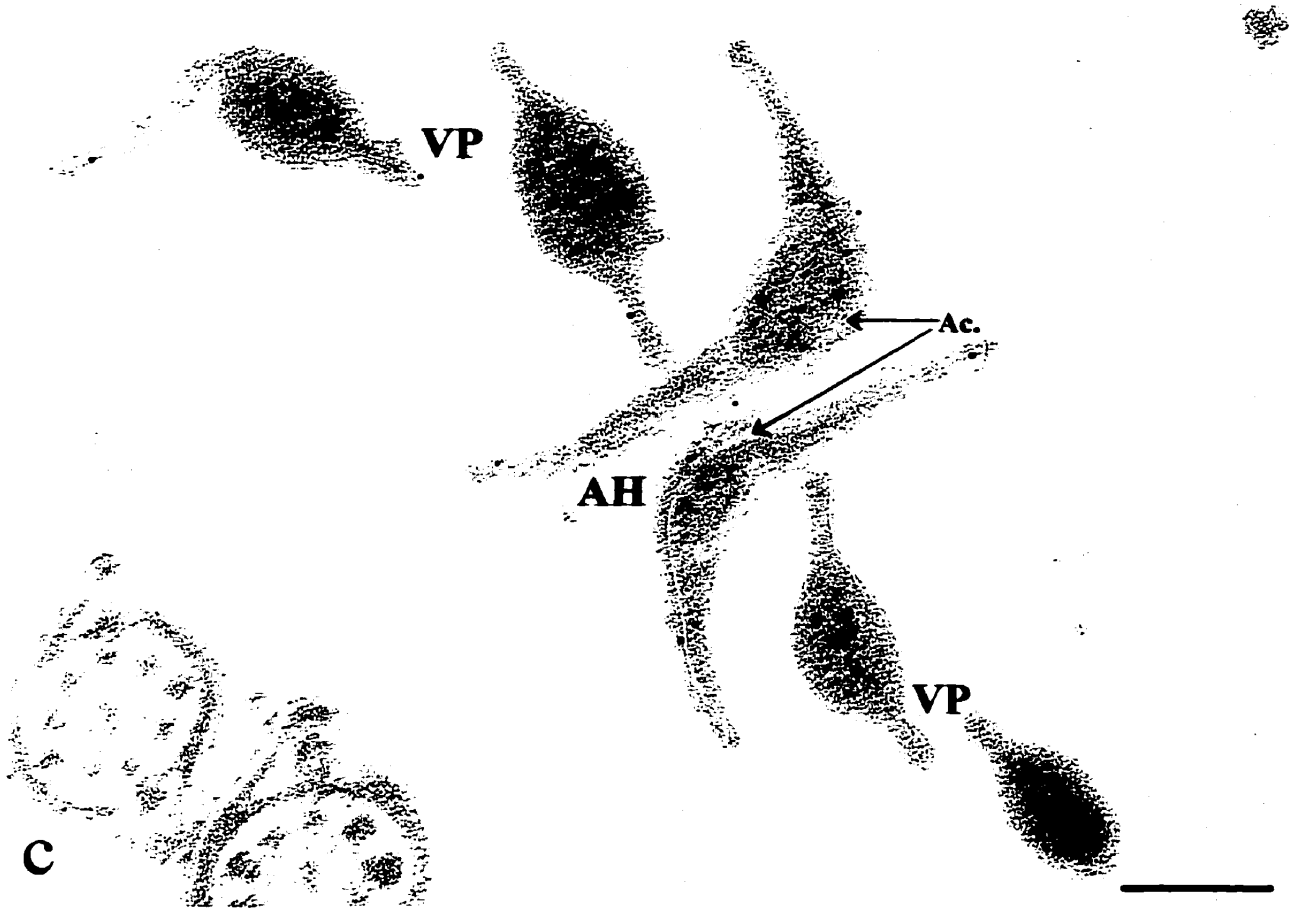
VP
Ac.
AH
VP
C

FIGURE 11 - Plains rat testicular sections immunogold labeled with anti-rat PERF antibodies all of which displayed identical patterns of labeling. **(a)** Sagital section of a step 10 early elongating spermatid, before descent of the manchette (M), labeled with anti-whole PERF antibody. Labeling appears in the spaces (S) corresponding to the subacrosomal layer. Note the nucleus (N) has not yet condensed and the abundance of labeling in the cytoplasm (Cyt.); arrows correspond to the nuclear ring. **(b)** Sagital section of Step 12 elongating spermatids immunogold labeled with anti-PERF15 antibody. Gold labeling is seen in the cytoplasm (Cyt.), along the manchette, and in the spaces (S) corresponding to the subacrosomal layer. Note the nucleus (N) is mostly condensed. **(c)** Sections of step 19 spermatids immediately after peforatorial protein condensation immunogold labeled with anti-whole PERF antibody. The cores of the VPs and the AH show abundant labeling. Ac., acrosome. Bars = 0.2 μm.


Ac.
M
S
S
M
Cyt.
a

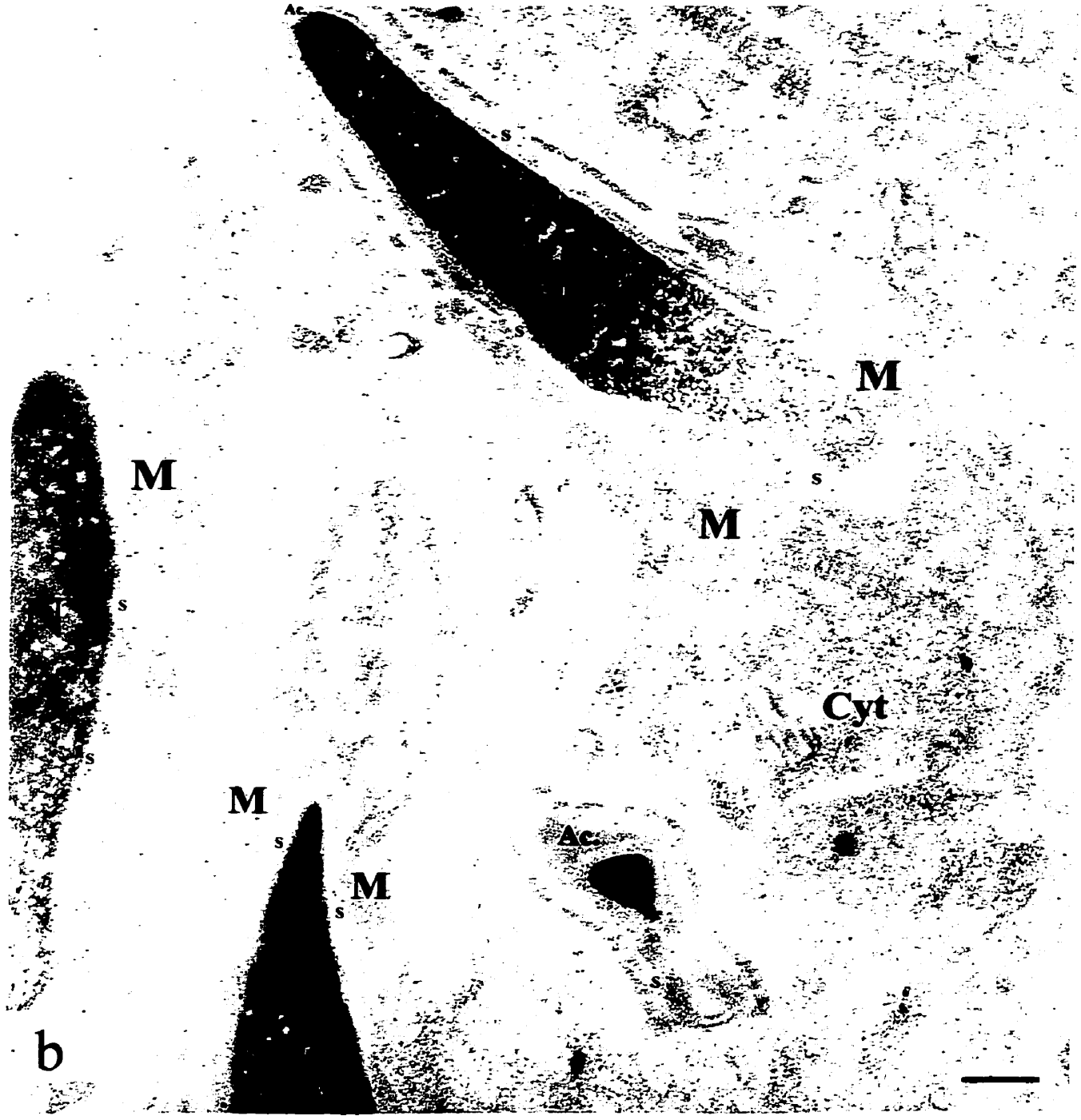
Ac
S
M
S
M
M
S
S
Cyt
M
S
M
S
Ac
S
b

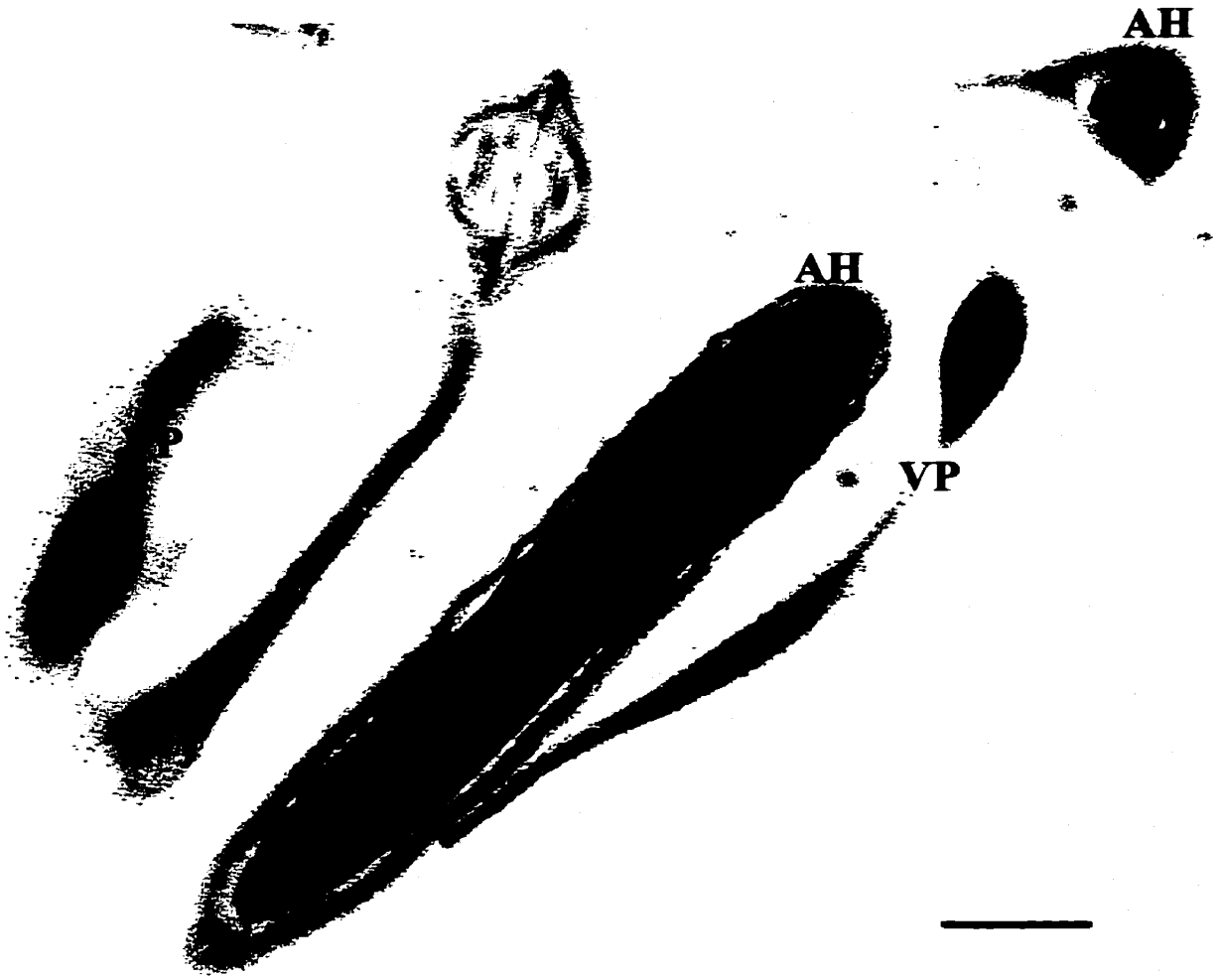

c

DISCUSSION

As far as we are aware the distribution and assembly of PERF has not yet been directly compared with PT proteins within the same species at the same time. In this study we have traced the testicular expression and assembly of these two groups of proteins in a sperm head type that has a very well developed cytoskeleton. By comparing the distribution of these proteins in the cytoskeleton of a spatulate shaped sperm head, a better understanding of the cellular events and processes involved in formation of the cytoskeleton may be achieved. For this study a murid species, the Plains rat, was identified that contained both sets of proteins. This species of murid, endogenous to Australia, evolved from a lineage that diverged from that which gave rise to the lab rat and lab mouse 15 to 20 million years ago. In the Plains rat, unlike in the lab rodent, there is in addition to an apical hook (AH), two ventral processes which extend from the upper concave surface of the sperm head (Breed, 1983, 1984; Flaherty and Breed, 1983). These processes each consist of a thick central core which is continuous with the perforatorium of the apical hook. The major proteins that were found in these processes are PERF 15 and actin (Breed *et al.*, 2000)

This study revealed that the alkaline extracted PERF-PT complex of the Plains rat is composed of many polypeptides, the most prominent of which has a molecular mass of 15 kDa. This polypeptide profile is very similar to that of the lab rat extracted PERF-PT complex (Fig. 3b) (Oko, 1995) and in both cases a lipid binding like protein PERF 15 (Oko and Morales, 1994) makes up most of the perforatorial core. On the other hand, bull sperm which has a spatulate head shape, lacks PERF 15 but contains another 15 kDa PT protein identified as a subacrosomal H2B variant, PT 15 (Aul and Oko, in press). We

provide evidence, by immunodetection, that PT 15 is also a constituent of the PT of the Plains rat and comigrates with PERF on SDS-PAGE. In fact, this study indicates that most of the PT proteins are common to both bull and Plains rat sperm. Thus the sperm head cytoskeleton of the Plains rat combines the protein compositional characteristics of both spatulate (bull) and falciform (rat, mouse) shaped sperm heads. What are then the distributional and developmental differences between these two different groups of the proteins (PT versus PERF) in the Plains rat sperm head? PERF proteins, in general, occupy the entire core of the AP and VPs and extend from these processes into the narrow subacrosomal region sandwiched between the acrosomal collar and the nucleus where they are present along with the PT proteins. However in the apical hook the PT proteins are restricted to the margins of the acrosome and nucleus while in the VPs they are only at the periphery of the separated acrosome head cap segments (SA). Some of the PT proteins, like PT 15, are restricted to the subacrosomal region of the PT while others, like PT 60 (Calicin) continue into the postacrosomal sheath (not shown) and still other PT proteins are exclusively postacrosomal (reviewed by Oko et al, 2001).

Perforatorial protein expression in the seminiferous epithelium of the Plains rat showed a similar temporal pattern to that of lab rat and mouse (Korely *et al.*, 1997; Oko and Clermont, 1991). There was a low level of expression of perforatorial proteins detected in the cytoplasm of mid-pachytene spermatocytes and round spermatids followed by an increase in cytoplasmic labeling in early elongating spermatids (steps 9-15) and finally an intense labeling in the cytoplasmic lobe of late elongating spermatids (steps 16-18). Most importantly, however, perforatorial proteins did not begin to enter the subacrosomal / periacrosomal region until step 8 spermatids just after the acrosome had

fully formed and was closely opposed to the nucleus. PT protein expression in the Plains rat testis, on the other hand, was associated with the forming acrosome and was similar to that found in the bull spermatids (Oko and Maravei, 1995). In the Plains rat, PT proteins were initially seen in steps 1-3 surrounding the forming acrosomic vesicle within the Golgi region and also during acrosome-nuclear docking throughout the cap phase of spermiogenesis (steps 4-7). Here PT proteins remained associated with the acrosomal membrane and formed the subacrosomal layer of the PT. In summary then, PERF proteins do not begin to enter the PT protein dominated subacrosomal region of murid sperm until step 8. In spatulate shaped sperm, such as the bull, this step of spermiogenesis would normally mark the end of subacrosomal formation. However, according to our ultrastructural analysis, a cytoplasmic recess which eventually retains a falciform shape begins to form within the subacrosomal layer and accommodates the PERF proteins which are transported up to this region in a yet unexplained way.

Considering that the apical hook of murids and the two falciform shaped VPs of the Plains rat are mostly composed of perforatorial proteins, it was tempting to hypothesize that the presence of the perforatorial proteins somehow facilitate the formation of the falciform shape of the sperm head. However, ultrastructural developmental analysis revealed that the framework for the existing falciform shape of the AP and VPs, was laid down between steps 8 and 16 of spermiogenesis well before the condensation of PERF proteins in this region to form the definitive perforatorial structures. These perforatorial structural changes and their timing in spermiogenesis of the Plains rat are in agreement to those previously shown in the lab rat by Lalli and Clermont (1981). Our immunocytochemical analysis and that of Oko and Clermont

(1991) in the lab rat suggest that, while the AP and VP structural changes occur during steps 8 and 16, the resulting spaces created are filled concomitantly with PERF proteins in a fluid state. The fact that condensation of these proteins does not occur until the very end of spermiogenesis (step 19) to form the rigid perforatorial structure suggests that perforatorial proteins do not dictate falciform shaping in the murid. Therefore we propose that PERF proteins are "filler proteins" analogous to clay filling a potter's mold.

What then would be responsible for the shape of the perforatorial structures? An obvious candidate for creating the framework of the AP and VPs would be filamentous actin as it is present in the subacrosomal region for most of spermiogenesis and is retained in the VPs of mature spermatozoa (Campanella *et al.*, 1979; Welch and O'Rand, 1985; Russell *et al.*, 1986; Halenda *et al.*, 1987; Flaherty *et al.*, 1988; Breed and Leigh, 1991; Oko *et al.*, 1991). In murids, it is first detected in the nascent subacrosomal layer of the round spermatids and continues to be present during the first steps of the maturation phase, only to disappear completely from this layer in the mature rat and mouse spermatozoa (Fouquet *et al.*, 1989). The co-localization of F-actin with PT and PERF proteins suggests a form of organized physical interaction. Recently, a major constituent of the bull and rat PT, PT 60 or Calicin, was shown to bind actin with high affinity and their co-localization to the subacrosomal layer during the greater part of spermiogenesis provides evidence for their physical interaction *in situ* (Lecuyer *et al.*, 2000). Another factor to be considered in the falciform shaping of the apical hook is the inherent apical shape change of the condensing murid sperm nucleus during the early elongation phase of spermiogenesis. The VPs, on the other hand, do not have a hooked shaped nuclear projection to conform to during their formation but rather a nuclear stump which

terminates near the base of these processes. In this case their actin filament network, which is retained in part after their development, may be crucial in setting up the hooked shape framework.

How do these perforatorial proteins find their way into this cytosolic space between the acrosome and nucleus and between the postacrosomal sheath and nucleus as in the Plains rat? The first hint of PERF proteins entering the subacrosomal region is at the end of round spermatid formation (step 8). It is at this time that the *manchette* forms, a transient cytoskeletal complex around the caudal half of the nucleus, just below the acrosome, by a sleeve of laterally associated microtubules that are attached at the equator (Fawcett *et al.*, 1971; Wolosewick and Bryan, 1977). Concurrently, the cell membrane at the posterior margin of the acrosomal cap becomes specialized to form a *nuclear ring*, into which the proximal ends of the microtubules of the manchette embed. The already formed acrosomal head cap which overlays the subacrosomal region and where it ends distally, proteins become laid down in the wake of the descending manchette forming the postacrosomal sheath of the PT (Oko and Maravei, 1995). Recently our lab has identified several proteins that are exclusive to the postacrosomal sheath that are transiently localized to the microtubules of the manchette during postacrosomal sheath assembly (Tovich et al; 2001, Oko *et al.*, 2001) implying that they use the manchette as a conduit to their site of assembly. Keeping in mind that the manchette links the end of the subacrosomal layer to the cytoplasmic lobe of the spermatid, and that its microtubules completely fill the cytoplasmic space between the sperm plasmalemma and nuclear envelope, it is logical to assume that the microtubules of the manchette would be involved in the transport of PERF proteins into the AP (see Figure 12 for schematic). In

fact, our immunolocalization analysis of PERF proteins show them to be associated with the microtubules of the manchette throughout the early elongation phase of spermiogenesis (steps 8-14). Since the VPs extend from a region where the acrosome cap ends it is possible that as the manchette descends and lays down the postacrosomal sheath it also channels the PERF proteins destined to fill the VPs. Since the manchette descends caudal to the nucleus and disappears by step 15 in the Plains rat, it is tempting to speculate that the transport of PERF proteins to their ultimate destination is complete by this time of spermiogenesis. To some degree this is supported by our immunocytochemical data showing PERF reactivity in the forming "cytosolic spaces" of the AP and VPs before step 15 of spermiogenesis.

ACKNOWLEDGMENTS

This work was supported by grants from the National Science and Engineering Research Council (R.O.) and the Australian Research Council (W.G.B.).

FIGURE 12 – Schematic illustrating the proposed theory of PERF protein transport into the subacrosomal layer (perforatorium) during spermiogenesis. The arrows indicate the manner in which the perforatorial proteins, which are initially in the cytoplasm (C), travel along the descending manchette (M) to ultimately reach the SL/perforatorial region. As a consequence of its descent, the M has laid down the postacrosomal sheath (PS) in its wake. The SL cytosolic space (outlined by arrowheads) becomes more defined with the development of the spermatid and gradually becomes filled with more PERF proteins that condense in the final step of spermiogenesis (Step 19) to form the perforatorium.. Nucleus, N; Ax., axoneme; Ac., acrosome (Picture from Russell *et al.*, 1990).

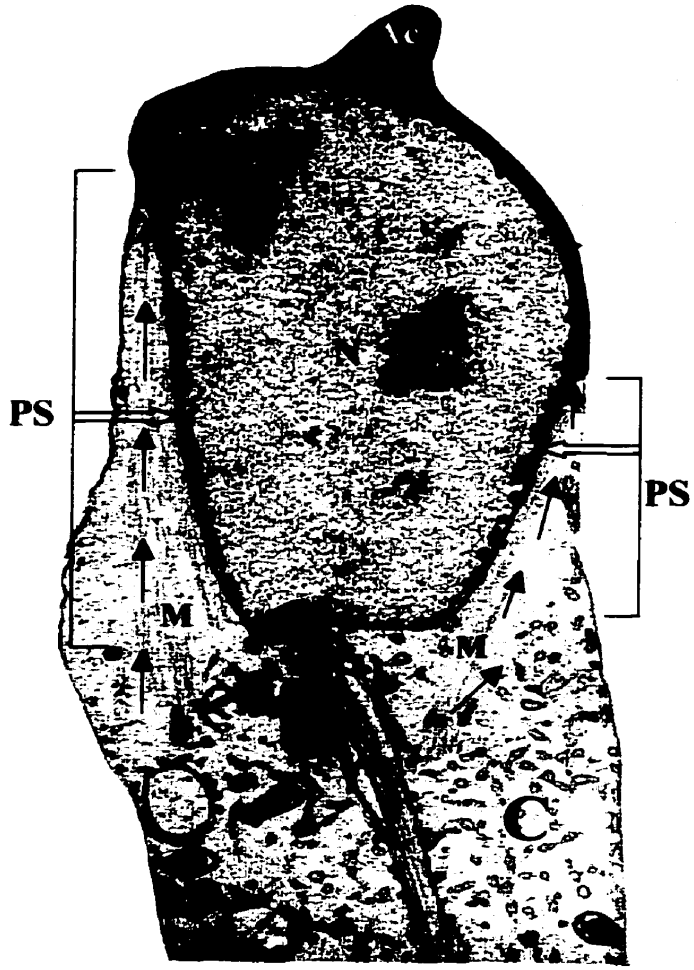
PS
PS
M
M

4. GENERAL DISCUSSION

The initial aim of this thesis was to determine the distribution of PERF and PT proteins in the cytoskeleton of the Plains rat sperm head. A comparison of the development of PT and PERF proteins has never been studied within the cytoskeleton of the same sperm head, thus for this study, we selected the Plains rat (*Pseudomys australis*) which has a greater development of the sperm head cytoskeleton than that of other mammalian species (Breed, 1983). The Plains rat spermatozoon has a unique sperm head morphology in which two falciform shaped ventral processes (VPs) extend from its upper concave surface, just inferior to the apical hook. In order to determine the developmental composition of both PT and PERF proteins within this model, we had to first verify the protein composition of these atypical VPs. As predicted, the VPs were shown to be perforatorial-like appendages that contain similar proteins to the AH of the lab rat, together with F-actin, the major constituent being PERF 15 while the PT proteins were restricted to areas close to the acrosomal and nuclear membranes.

Developmental studies are crucial for determining both the temporal expression as well as ascertaining the spatial association and expression of these two sets of proteins in the Plains rat. Figure 13 summarizes these findings (adapted from Dym and Clermont, 1978). Although this diagram has been adapted from the lab rat cycle of the seminiferous epithelium, it has been used as a reference for staging throughout this thesis for the purpose of comparing, temporally, PERF and PT protein expression and assembly during spermiogenesis due to assembly similarities between the two animals.

As seen in Figure 12, spermiogenesis was divided into two major phases based upon the developmental expression of two groups of perinuclear theca proteins: (a) the

PT subacrosomal layer assembly of PT proteins and (b) the perforatorial core assembly of PERF proteins. In the first phase, step 1, the PT proteins appear as they surround the acrosomic vesicle and continue their association with the acrosome development throughout the rest of spermiogenesis. At step 7, the PT assembly and its permanent acrosomic and outer periacrosomic layer associations are finalized when acrosomic development is complete and sperm head morphological changes begin. The second phase is the perforatorial core assembly, which is more intricate and has been divided into three major sections. The first, from step 8 to step 14, is the PERF protein transport period which is when the already translated PERF proteins begin to relocate, from the cytoplasm to the perforatorial core regions of the AH and VPs. The second phase, from steps 15-18, describes the final shape changes and interim period before perforatorial condensation occurs. The final phase, step 19, is the time when condensation of perforatorial proteins occurs.

The plains rat sperm head provided a model in which both PT and PERF proteins occur and from this study we conclude that PT proteins are the fundemental set of proteins associated with acrosomal assembly, in both the falciform and spatulate shaped sperm heads, whereas the PERF proteins serve as "filler" proteins of a falciform shaped sperm whose shape has already been predetermined. The latter is seen in both the AH of all falciform shaped sperm heads and the VPs of Australian rodents.

In our second aim, we wished to determine whether there are differences in protein profiles of the cytoskeleton of the Plains rat sperm head from that in two species that have a spatulate shaped sperm head. Previously, the PERF proteins have only been

found to occur in the perforatorium of the AH of the lab rat and lab mouse sperm head (Lalli and Clermont, 1981, Oko, 1995) and now also in the VPs of the Plain rat sperm, whereas PT proteins are found in sperm of most studied eutherian mammals (Breed, 1997). In this present investigation, the bull was chosen as the example of a spatulate shaped sperm head, and as expected, PERF proteins were not found in the bull sperm head PT (Aul and Oko, in press), suggesting the view that PERF proteins are murid specific. Study of the perinuclear theca of a murid with a spatulate sperm head would perhaps show whether PERF proteins occurred in a murid sperm head due to its hooked shape or was a characteristic of murid sperm heads regardless of shape. We, therefore, also carried out a preliminary investigation of the sperm head of a Southern Asian rodent, *Bandicota indica*. The sperm of this species is most unusual in having a bulbous head morphology. Preliminary studies on the developmental aspect of PT versus PERF proteins were performed on sperm of this species (see Appendix C). Based on its sperm head shape, which is more similar to that of the bull spatulate sperm head, and on the assumption that PERF only occurs in a falciform sperm head, we hypothesized that PT proteins but not PERF proteins would be found within the *Bandicota indica's* perinuclear theca. However, to our surprise, both PT and PERF proteins were found within it. The PT developmental assembly revealed the immunoperoxidase reaction to be first seen early in step 3 surrounding the acrosomic vesicle (Appendix C, Fig. 1a), followed by a continued association with the developing acrosome (Appendix C, Fig, 1b), which corresponds to what was seen in the bull, lab rat and Plains rat. The PERF protein assembly, on the other hand, showed an initial appearance is around step 5 of spermiogenesis, a little earlier than that seen in the two species of rats studied, which occurred at step 8 (Appendix C, Fig 2).

These results raised several interesting points. (1)that the non-falciform sperm head of a rodent, *Bandicota indica*, has, unlike that of the bull, the presence of PERF proteins; (2) that the murid sperm head cytoskeleton have PERF proteins present regardless of whether the sperm head shape is falciform or conical; (3) that PERF proteins are not the cause of the hook shaped sperm head of murid rodents; (4) PT proteins are present and associated with the acrosome throughout development, regardless of sperm head shape.

In our final aim, we wished to determine whether there was a correlation between sperm head shape and the presence of the two established groups of cytoskeletal proteins, PERF and PT. As alluded to previously, there are two common sperm head shapes that exist within eutherian mammals: spatulate shape, as seen in the bull sperm head, and falciform shape, as seen in laboratory rat sperm heads. With this in mind, it was important to decide which of the three major components of the sperm head (the nucleus, the acrosome or the perinuclear theca) might determine the sperm head shape. However, the nucleus can be discounted in determining nuclear shape because it condenses early in spermiogenesis before shaping of the sperm head develops, whereas the acrosome contains acid hydrolases and other enzymes that are involved in fertilization processes (reviewed by Fawcet, 1975). Therefore, by process of elimination, the perinuclear theca may, in some way, influence sperm head shape that develops not only because it is localized to the area between the nucleus and acrosome, but also because it is a cytoskeletal element that is co-localized with actin microfilaments throughout the development of most mammalian spermatozoa (Campanella *et al.*, 1979; Welch and

O'Rand, 1985; Russell *et al.*, 1986; Halenda *et al.*, 1987; Flaherty *et al.*, 1988; Breed and Leigh, 1991; Oko *et al.*, 1991).

Although we had hoped that our investigation would indicate an answer to the cause of sperm head shaping, we found no correlation between sperm head shape and the presence of the PERF in hook shaped sperm heads. Instead we found that there was a universal presence of PT proteins in the eutherian mammals studied, as well as the presence of PERF proteins in the sperm head cytoskeleton of all murids studied in the investigation, even when the head shape was non-falciform murids.

The mechanisms underlying the cause behind sperm head shaping still remain unknown and until the entire eutherian sperm head protein cytoskeleton composition is determined and its function characterized, it will remain to be seen how the final form of the sperm head shape is brought about.

FIGURE 13 – Summary diagram of PERF and PT subacrosomal layer assembly throughout the stages of the Cycle of Plains Rat seminiferous epithelium (Adapted from Dym and Clermont, 1968). Assembly of both PERF and PT proteins occurs during Spermiogenesis, however, they do so at separate times and the entire event can be described through four phases. First is the PT protein SL assembly which begins at step 1 of spermiogenesis and ends at about step 7; the protein is associated with the acrosome as it resides in the SL. The second phase is PERF protein SL assembly which begins at step 8, but with very little presence in the SL, and continues into the transport phase at about step 13. This third phase highlights PERF protein transfer and its presence in much larger quantities in the SL. The final phase is PERF protein condensation which occurs in the last step of spermiogenesis (step 19), forming the rigid cytoskeletal perforatorium.

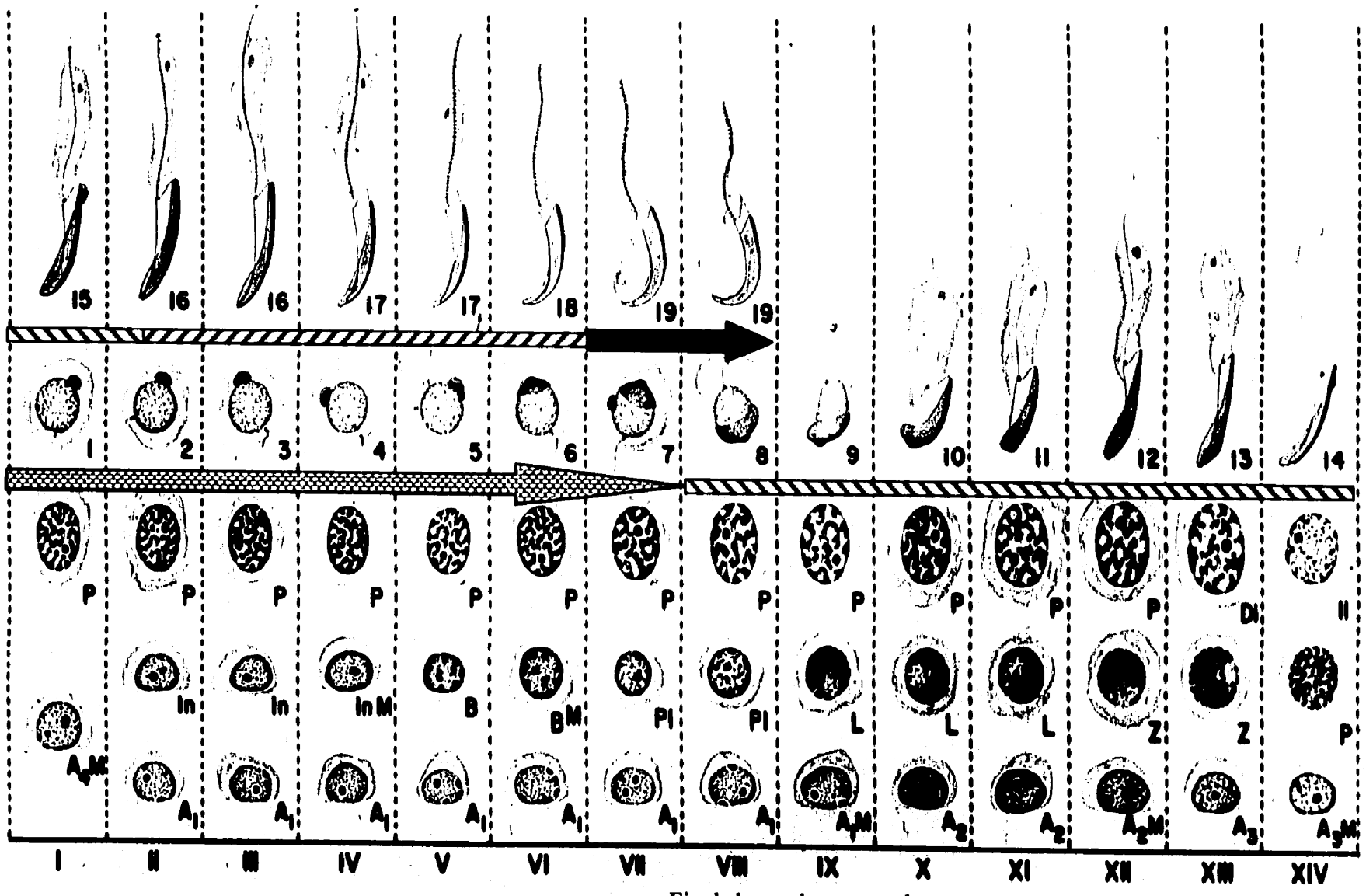

(Adapted from Dym and Clermont, 1978)

REFERENCES

Aul, B.R. and R. Oko (in press) The major subacrosomal occupant of bull spermatozoa is a novel H2B varient (SubH2Bv) associated with the forming acrosome during spermiogenesis. *Developmental Biology*.

Balhorn, R., S. Weston, C. Thomas and A. Wyrobek (1984) DNA packaging in mouse spermatids. Synthesis of protamine variants and four transition proteins. *Exp. Cell Res.* **150** : 298-308.

Barth, A.D. and R.J. Oko (1989) Normal Bovine Spermatogenesis and Sperm Maturation. *In:* Abnormal Morphology of Bovine Spermatozoa. p. 19-49. Iowa State University Press, Iowa.

Bedford, J.M. (1991) The coevolution of mammalian gametes. In 'A Comparative Overview of Mammalian Fertilization'. (Eds B.S. Dunbar and M.G. O'Rand.) pp.3-30 Plenum Press, New York.

Bishop M.W.H. and C.R. Austin (1957) Mammalian spermatozoa. *Endeavour* **16** : 137-150.

Bishop M.W.H. and A. Walton (1960) Spermatogenesis and the structure of mammalian spermatozoa. In: Parkes AS (ed.), Marshall's Physiology of Reproduction, vol.1, 3rd ed. London: Longmans; pp.1-29.

Breed, W.G. and V. Sarafis (1979) On the Phylogenetic significance of spermatozoal morphology and male reproductive tract anatomy in Australian rodents. *Trans R Soc S Aust.* **103** : 127-139.

Breed, W.G. (1982) Morphological variation in the testes and accessory sex organs of Australian rodents in the genera *Pseudomys* and *Notomys*. *J Reprod Fertil.* **66** : 607-613.

Breed, W.G. (1983) Variation in sperm morphology in the Australian rodent genus, *Pseudomys* (Muridae).*Cell Tissue Research.* **229** : 611-625.

Breed, W.G. (1984) Sperm head structure in the *Hydromyinae* (Rodentia: Muridae): a further evolutionary development of the subacrosomal space in mammals. *Gamete Reseeach.* **10** : 31-44.

Breed, W.G. (1986) Comparitive morphology and evolution of the male reproductive tract in the Australian Hydromyine rodents (Muridae). *J Zool. Lond* (A) **209** : 607-629.

Breed, W.G., Swift J.G. and T.M. Mukherjee (1988) Variation in intramembranous particle distribution in the cell membrane of the sperm head of the plains rat and western chestnut mouse (*Pseudomys* Spp.) *J. Submicrosc. Cytol. Pathol.* **20** : 341-348.

Breed, W.G. and C.M. Leigh (1991) Distribution of Filamentous Actin in and Around Spermatids and In Spermatozoa of Australian Conilurine Rodents. *Molecular Reproduction and Development* **30** : 369-384.

Breed, W.G. (1993) Novel organization of the spermatozoon in two species of murid rodents from Southern Asia. *Journal of Reproduction and Fertility*. **99** : 149-158.

Breed, W.G. (1997) Evolution of the Spermatozoon in Australasian Rodents. *Australian Journal of Zoology*. **45** : 459-478.

Breed W.G., Idriss D, and R. Oko (2000) Protien composition of the Ventral Processes on the Sperm Head of Australian Hydromyine Rodents. *Biology of Reproduction*. **63** : 629-634.

Clermont Y., and C.P. Leblond (1952) Spermiogenesis of Man, Monkey, Ram, and Other Mammals as shown by the "Periodic Acid-Schiff" Technique. *American Journal of Anatomy*. **118** : 509-524.

Clermont Y., Eingerg E., Leblond C.P., and S. Wagner (1955) The Peforatorium – An Extension of The Nuclear Membrane of the Rat Spermatozoon. *The Anatomical Record*. **121** (1) : 1-12.

Clermont, Y. and E. Bustos-Obregon (1968) Re-examination of spermatogoinal renewal in the rat by means of seminiferous tubules mounted "in toto." *American Journal of Anatomy*. **122**: 237-248.

Clermont, Y. (1972) Kinetics of Spermiogenesis in Mammals: Seminiferous Epithelium Cylce and Spermatogonial Renewal. *Physiological Reviews*. **52** (1) :198-236.

Cole A., Meistrich M.L., Cherry LM., and P.K. Trostle-Weige (1988) Nuclear and Manchette Development in Spermatids of Normal and *azh/azh* Mutant Mice. *Biology of Reproduction*. **38** : 385-401.

Courot M, M.T Hochereau-de Reviers, and R. Ortavant (1970) Spermatogenesis. *In:* The Testis: Development, Anatomy and Physiology. (A.D. Johnson, W.R. Gomes and N.L Vandemark. Eds), p.339-432. Academic Press, New York.

Evrette, N.B. (1945) The present status of the germ-cell problem in vertebrates. *Biol. Rev.* **20**: 45.

Fawcett D.W., Anderson W.A., and D.M. Phillips (1971) Morphogenetic Factors Influencing the Shape of the Sperm Head. *Developmental Biology*. **26** : 220-251.

Fawcett, D.W. (1975) Review Article: The Mammalian Spermatozoon. *Developmental Biology*. **44** : 394-436.

Flaherty, S.P. and W.G. Breed (1983) The sperm head of the plains mouse *Pseudomys australis*: ultrastructure and effects of chemical treatments. *Gamete Research.* **8** : 231-244.

Flaherty S.P., W.G. Breed and V. Sarafis (1983) Localization of actin in the sperm head of the plains mouse, *Pseudomys australis*. *J Exp. Zoology.* **225** : 497-500.

Flaherty, S.P. (1987) Further Ultrastructural Observations on the Sperm Head of the Plains Mouse, *Pseudomys australis* (Rodentia: Muridae) *The Anatomical Record.* **217** : 240-249.

Flaherty S.P. and W.G. Breed (1987) Formation of the Ventral Hooks on the Sperm Head of the Plains Mouse, *Pseudomys australis*. *Gamete Research* **17** : 115-129.

Flaherty S.P., Winfrey V.P., and F.E. Olson (1988) Localization of Actin in Human, Bull, Rabbit, and Hamster, Sperm by Immunoelectron Microscopy. *The Anatomical Records.* **221** : 599-610.

Flannery, T. (1995) Mammals of New Guinae. Chatswood, NSW: Reed Books; pp. 1-568.

Fouquet F.P., Kann M.L., and J.P. Dadoune (1989) Immunogold Distribution of Actin During Spermiogenesis in the Rat, Hamster, Monkey, and Human. *The Anatomical Record.* **223** : 35-42.

Friend, G.F. (1936) The Sperms of British Muridae. *Q J Microsc. Sci.* **78** : 419-443.

Halenda R.M., Primakoff P., and D. Gold Myles (1987) Actin Filaments, Localized to the Region of the Developing Acrosome during Early Stages, Are Lost during Later Stages of Guinae Pif Spermiogenesis. *Biology of Reproduction* **36** : 491-499.

Hand, S. (1984) Australia's oldest rodents – master mariners from Malaysia. In: Archer M., Clayton G. (eds), Vertebrate Zoogeography and Evolution in Australia. Carlisle, Western Australia: Hesperian Press; pp. 905-912.

Hecht, N.B. (1987) Gene expression during spermatogenesis. *Ann. N.Y. Acad. Sci.* **513** : 90-101.

Huckins, C. (1971) The spermatogonial stem cell population in adult rats. I. Their Morphology, proliferation, and maturation. *Anat. Rec.* **169**: 533-558.

Irons, M.J., and Y. Clermont (1982) Formation of outer dense fibers during spermiogenesis in the rat. *Anat Rec.* **202** : 463-471.

Irons, M.J., and Y. Clermont (1982) Kinetics of fibrous sheath formation in the rat spermatid. *Am. J. Anat.* **165** : 121-130.

Irons, M.J. (1983) Synthesis and assembly of connecting-piece proteins as revealed by radioautography. *J. Ultrastruct. Res.* **82** : 27-34.

Korley R, Pouresmaeili F, and R. Oko (1997) Analysis of the Protein Composition of the Mouse Sperm Perinuclear Theca and Characterization of Its Major Protein Constituent. *Biology of Reproduction.* **57** : 1426-1432.

Laemmli, V.K. (1970) Cleavage of structural proteins during the assembly of the heads of bacterophage T4. *Nature* **227** : 680-685.

Lalli M., and Y. Clermont (1981) Structural Changes of the Head Components of the Rat Spermatid During Late Spermiogenesis. *The American Journal of Anatomy.* **160** : 419-434.

Leblond C.P., and Y. Clermont (1952) Spermiogenesis of Rat, Mouse, Hamster, and Guinae Pig as Revealed by the "Periodic Acid-Fuchsin Sulfurous Acid" Technique. *The American Journal of Anatomy.* **90** (2) : 167-215.

Lecuyer C., Dacheux J.L., Hermand E., Mazeman E., Rousseaux., and R. Rousseaux-Prevost (2000) Actin-Binding Properties and Colocalization with Actin During Spermiogenesis of Mammalian Sperm Calicin. *Biology of Reproduction.* **63** : 1801-1810.

Lee, A.K., P.R. Baverstock and C.H.S. Watts (1981) Rodents – the late invaders. InL Keast A (ed.), Ecological Biogeography of Australia, vol. 3. The Hague: Junk; pp,1521-1553.

Lessard, JL (1988) Two monoclonal antibodies to actin: one muscle selective and one generally reactive. *Cell Motil Cytoskeleton.* **10** : 349-362.

Loir, M., and Lanneau M. (1984) Structural function of the basic nuclear proteins in ram spermatids. *J. Cell Biol.* **86** : 262-276.

Lora-Lamia, C., Castellani-Ceresa L., Andreetta F., Cotelli F., and M. Brivio (1986) Localization and Distribution of Actin in Mammalian Sperm Heads. *Journal of Ultrastructure and Molecular Structure Research.* **96** : 12-21.

Masri, B.A., L.D. Russell and A.W. Vogl (1987) Distribution of actin inspermatids and adjacent Sertoli cell regions of the rat. *Anat Rec.* **218** : 20-26.

McGadey, J. (1970) A tetrazolium method for non-specific alkaline phosphatase. *Histochemie.* **23** : 180-184.

Mintz, B. (1959) Continuity of the female germ cell line from embryo to adult. *Arch. Anat. Microscopy Mophol. Exptl.* **48** bis, 155.

Mintz, B. (1960) Embryological phases of mammalian gametogenesis (Symposium on mammalian genetics and reproduction). *Journal of Cellular Comp. Physiol.* **56**, Suppl. 1,31.

O'Brien D.A., and A.R. Bellve (1980) Protein Costituents of the Mouse Spermatozoon I: An Electrophoretic Characterization. *Developmental Biology.* **75** : 386-404.

Oko R, and Y. Clermont (1988) Isolation, Structure and Protein Composition of the Perforatorium of Rat Spermatozoa. *Biology of Reproduction.* **39** : 673-687.

Oko R., Moussakova L., and Y. Clermont (1990) Regional Differences in Composition of the Perforatorium and Outer Periacrosomal Layer of the Rat Spermatozoon as Revealed by Immunocytochemistry. *The American Journal of Anatomy.* **188** : 64-73.

Oko R, and Y. Clermont (1991) Biogenesis of Specialized Cytoskeletal Elements of Rat Spermatozoa. *Annals of the New York Academy of Sciences.* **637** : 203–223.

Oko R., and Y. Clermont (1991) Origin and Distribution of Perforatorial Proteins During Spermatogenesis of the Rat: An Immunocytochemical Study. *The Anatomical Record.* **230** : 489-501.

Oko R., Hermo L., and N.B. Hecht (1991) Distribution of Actin Isoforms Within Cells of the Seminiferous Epithelium of the Rat Testis: Evidence for a Muscle Form of Actin in Spermatids. *The Anatomical Record.* **231** : 63-81.

Oko R. and D. Maravei (1994) Protein composition of the perinuclear theca of bull spermatozoa. *Biol. Reprod.* **50** : 1000-1014.

Oko R., and C.R. Morales (1994) A Novel Testicular Protein, with Sequence Similarities to a Family of Lipid Binding Proteins, Is a Major Component of the Rat Sperm Peinuclear Theca. *Developmental Biology.* **166** : 235-245.

Oko R. and D. Maravei (1994) Protein composition of the perinuclear theca of bull spermatozoa. *Biol. Reprod.* **50** : 1000-1014.

Oko, R. (1995) Developmental expression and Possible Role of Perinuclear Theca Proteins in Mammalian Spermatozoa. *Reprod. Fertil. Dev.* 7 : 777-797.

Oko R., and D. Maravei (1995) Distribution and Possible Role of Perinuclear Theca Proteins During Bovine Spermiogenesis. *Microscopy Research and Technique.* **32** 520-532.

Oko, R., R.B. Aul, A. Wu and P. Sutovsky (2001) The Sperm Head Cytoskeleton. *In:* Andrology in the 21st Century: Proceedings of the VII International Congress of Andrology. (eds. B. Robaire, H.Chemes and C.R. Morales) pp.37-51. Medimond Publishing Company, New Jersey.

Olson G.E., Hamilton D.W., and D.W. Fawcette (1976) Isolation and Characterization of the Perforatorium of the Rat Spermatozoa. *Journall of Reproduction and Fertility.* **47** : 293-297.

Pierce, E.J. and W.G. Breed (1989) Light microscopical structure of the excurrent ducts and distribution of spermatozoa in the Australian rodents, *Pseudomys australis* and *Notomys alexis. J Anat.* **162** : 195-213.

Piko L. (1969) Gamete structure and sperm entry in mammals. In: Metz CB, Monroy A (eds.), Fertilization. New York and London: Academic Press; pp. 325-403.

Pouresmaeili F., Morales C.R., and R. Oko (1997) Moleculalr Cloning and Structural Analysis of the Gene Encoding PERF 15 Protein Present in the Perinuclear Theca of the Rat Spermatozoa. *Biology of Reproduction.* **57** : 655-659.

Russell, L.D., R.A. Etllin, A.P Sinha Hikim and E.D. Clegg (1970) Mammalian Spermatogenesis. *In*: Histological and Histopathological Evaluation of the Testis. p. 1-38. Cache River Press, Florida.

Russel L.D., Weber J.E., and A.W. Vogl (1986) Characterization of Filaments within the Subacrosomal Space of Rat Spermatids During Spermiogenesis. *Tissue and Cell.* **18** (6) : 887-898.

Strahan, R. (1995) The Mammals of Australia. Chatswood, NSW: Reed Books; pp. 1-756.

Talian JC, Olmsted JB, and R.D. Goldman (1983) A Rapid preocedure for preparing fluorescein labeled specific antibodies from whole antiserum: its use in analyzing cytoskeletal architecture. *J Cell Biol.* **97** : 1277-1282.

Thorne-Tjomsland, G., Y. Clermont and L. Hermo (1988) Contribution of the Golgi apparatus componenets to the fomation of the acrosomic system and chromotoid body in rat spermatids. *Anat. Rec.* **221** : 591-598.

Tovich, P.R., M. Oda, Y. Yu and R. Oko (2001) Isolation and Perinuclear Immunolocalization of Somatic Histones H2B and H3 in Bull Sperm Heads. *Journal of Andrology Suppl.* P3/4-004, p. 119.

Vogl, A.W., B.D. Grove and G.J. Lew (1986) Distribution of actin in Sertoli cell ectoplasmic specializations and associated spermatids in the ground squirrel testis. *Anat Rec.* **215** : 331-341.

Watts, C.H.S and P.R Baverstock (1995) Evolution of the Murinae (Rodentia) as assessed by microcomplement fixation of albumen. *Aust J Zool.* **43** : 105-118.

Welch J.E, and M.G. O'Rand (1985) Identification and Distribution of Actin in Spermatogenic Cells and Spermatozoa of the Rabbit. *Developmental Biology.* **109** : 411-417.

APPENDIX

APPENDIX A

Linear gradient SDS polyacrylamide gel of bull and rat perinuclear theca (PT) polypeptides stained with Coomassie blue dye. *Lane S*, the molecular weight standards (x 1000). *Lane R*, rat PT polypeptides obtained from the final extraction step in 100 mM NaOH. *Lane B*, bull PT polypeptides obtained from the final step of NaOH; the six designated bands are the most prominent. Note that the protein profiles of the rat and bull PT polypeptides are similar, but in the case of the rat the 15 kDa PT polypeptide (PERF 15) dominates (adapted from Oko review, 1995).

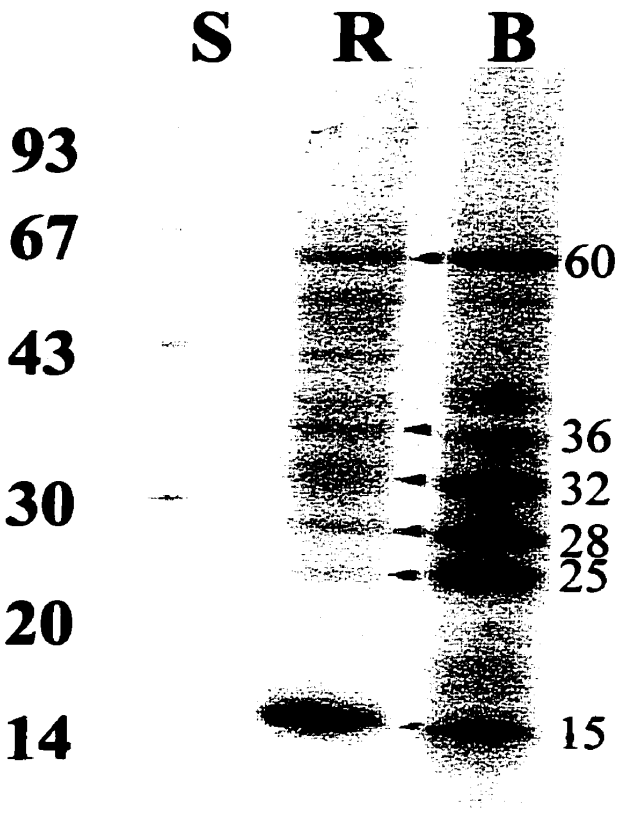
S
R
B
93
67
43
30
20
14
60
36
32
28
25
15

APPENDIX B

Spermiogenesis of both the rat **(i)** and the bull **(ii)** illustrates the transformation of the most immature spermatid (step 1 in both) into a spermatozoon (step 19 in the rat, step 14 in the bull). The schematic has been divided into the four phases of spermiogenesis for both species; note that each phase has the same characteristics for both the rat and the bull, however the duration of these phases varies between the two species. The Golgi phase is the time from the formation of the round spermatid (step 1) until the formation of spherical acrosomic granule associated with the nucleus (step 3 in both). The cap phase is delineated by the spermatids that have a growing acrosomic head cap (steps 4-7 in both), while the phase in which the nucleus and acrosome undergo the most dramatic transformations (ie. Condensation, elongation and shaping) is the acrosomic phase (step 8-12 in the bull, 8-14 in the rat). The maturation phase consists of spermatids that are completing their differentiation which includes the final formation of the tail and neck-piece along with final condensation of the nucleus (steps 13-14 in the bull, steps 15-19 in the rat). Note the rat spermiogenic diagram is adapted from Clermont and Rambourg , 1978, while the bull was adapted from Barth and Oko, 1990.

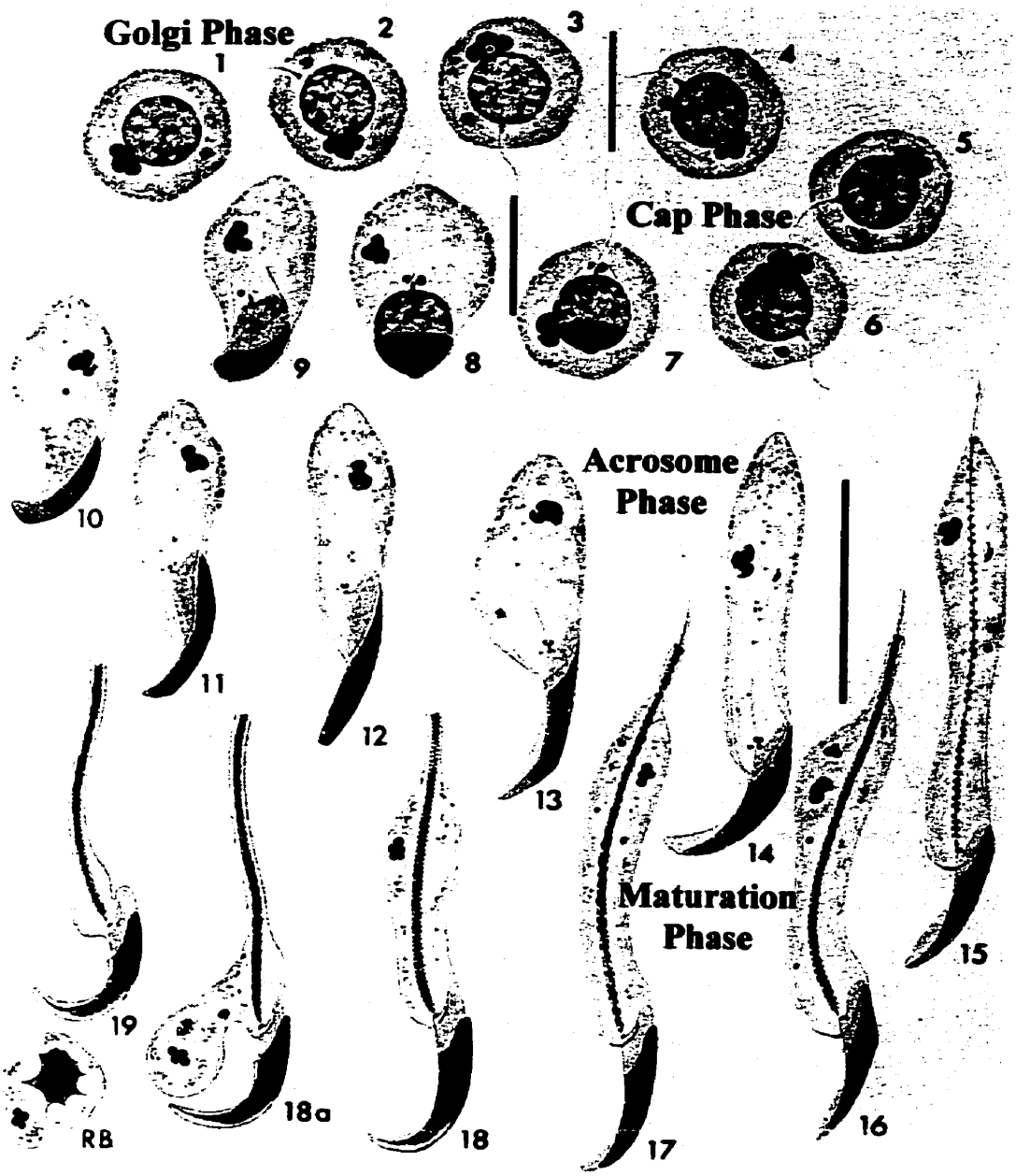

Appendix B (i) – Rat spermiogenesis and its four phases.
RB, residual body. Adapted from Clermont and Rambourg (1978).

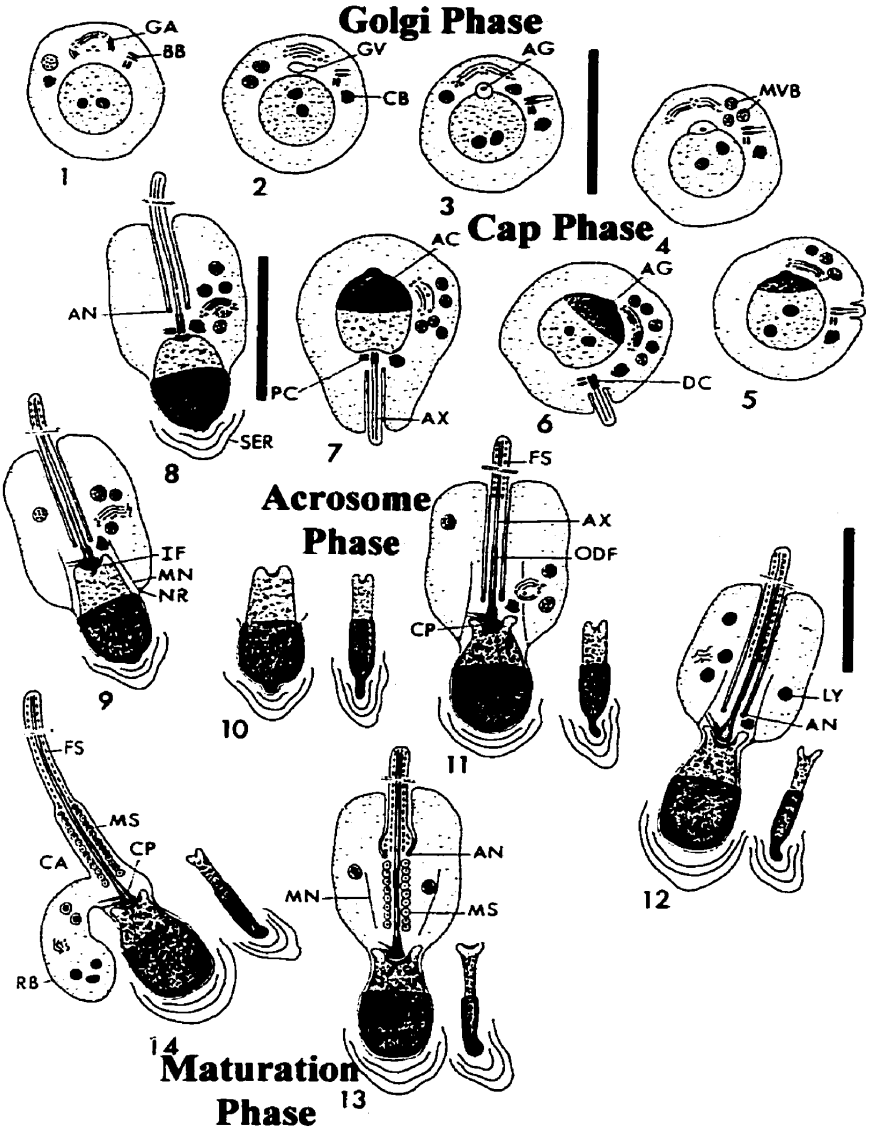

Appendix B (ii) - Bull spermiogenesis and its four stages; GA, Golgi Apparatus; (GV) Golgi vesicle; CB, chromatoid body; AG, acrosomic Granule; PC/DC; proximal/distal centriole; AN, annulus; AX, axoneme; IF, implantation fossa; MN, manchette; NR, nuclear ring; FS fibrousSheath; ODF, outer dense fibers; CP, capitulum; MS, mitochondrial Sheath; RB, residual body; CP, connecting piece. Adapted from Barth and Oko, 1990.

APPENDIX C

INTRODUCTION

The head of a spermatozoon belonging to eutherian mammals characteristically has a nucleus with a haploid set of chromosomes, an acrosomal cap and a cytoskeletal element. The majority of these mammals have a spatulate shape, the bull being an excellent representative, while most rodents have the typical falciform shape seen in a lab rat or lab mouse. However, the evolution of the Order Rodentia is interesting and there is great diversity between species in sperm head shape (Breed, 1997).

We were particularly interested in a genus found in Southeast Asia, *Bandicota*, two species of which have been shown to have an unusual rodent sperm head morphology which is bulbous and globular in shape. It lacks a narrow and well-defined apex or a clearly delineated perforatorium, as seen in both the laboratory rat, Plans rat (*Pseudomys* australis) and several other murid rodent species (Breed, 1993). Immunocytochemical studies have been carried out on cauda epididymal spermatozoa of two *Bandicota* species, *Bandicota indica and Bandicota savilei.* For the purpose of our investigation, primarily based on availability of tissue, we decided to use the former for our studies.

The nucleus of the *Bandicota indica*, was normal in appearance and was capped by a huge globular acrosome. Its shape varied and at times there were one or two nuclear extensions into invaginations of the inner acrosomal membrane. The equatorial segment of the acrosome could not be found, the subacrosomal layer was usually a very narrow space with occasional small apical projections, and the postacrosomal sheath being small in comparison to that of the lab rat spermatozoa (Breed, 1993).

Due to its shape and lack of a typical murid falciform shape, we hypothesized the developmental localization and assembly of perinuclear theca proteins of the *Bandicota indica* sperm, will most likely be similar to those of the bull rather than the lab rat. That is, antibodies raised against the entire bull-PT and anti-PT15/SubH2Bv will be present and display the same localization and developmental pattern in spermatogenesis as they had found in the bull (Oko and Maravei, 1995). The antibodies against the lab rat perforatorium and against PERF-15 will most likely be absent due to the lack of a typical perforatorial structure. What we found in our initial studies was quite interesting.

METHODS AND MATERIALS

Immunocytochemistry

Testes and caudae epididymides were obtained from *Bandicota indica* obtained in central Thailand. Each animal was killed and small pieces of testes and caudae epididymides were removed and immersed in 3% glutaraldehyde-3% fomaldehyde made up in a phosphate buffer. Ultra-thin sections were cut and mounted on formivar grids, which were subject to appropriate antibodies (as described in Idriss *et al.*, 2001), followed by staining with uranyl acetate and lead citrate and viewed via Transmission Electron Microscopy.

Testes were obtained, fixed for paraffin sections, subjected to the above antibodies and stained as described in Idriss *et al.*, 2001. These slides were mounted using parmount and then viewed via Light Microscopy.

FIGURE 1 – Immunoperoxidase staining of *Bandicota indica* seminiferous tubules using the ABC method. Note that both anti-whole PERF and anti-PERF 15 labelled in the same manner. **(a)** Anti whole-PERF antibody (4442) indicating labelling of the spermatid population (the reaction is associated with the SL layer demarcating the sperm head bulbous nature) **(b)** Anti-PERF 15 antibody revealing initial SL assembly of PERF proteins occurs at step 4 as indicated by the acrosome association (arrowheads); this is earlier than the lab rat which occurs at step 8. Bars = 10 μm.

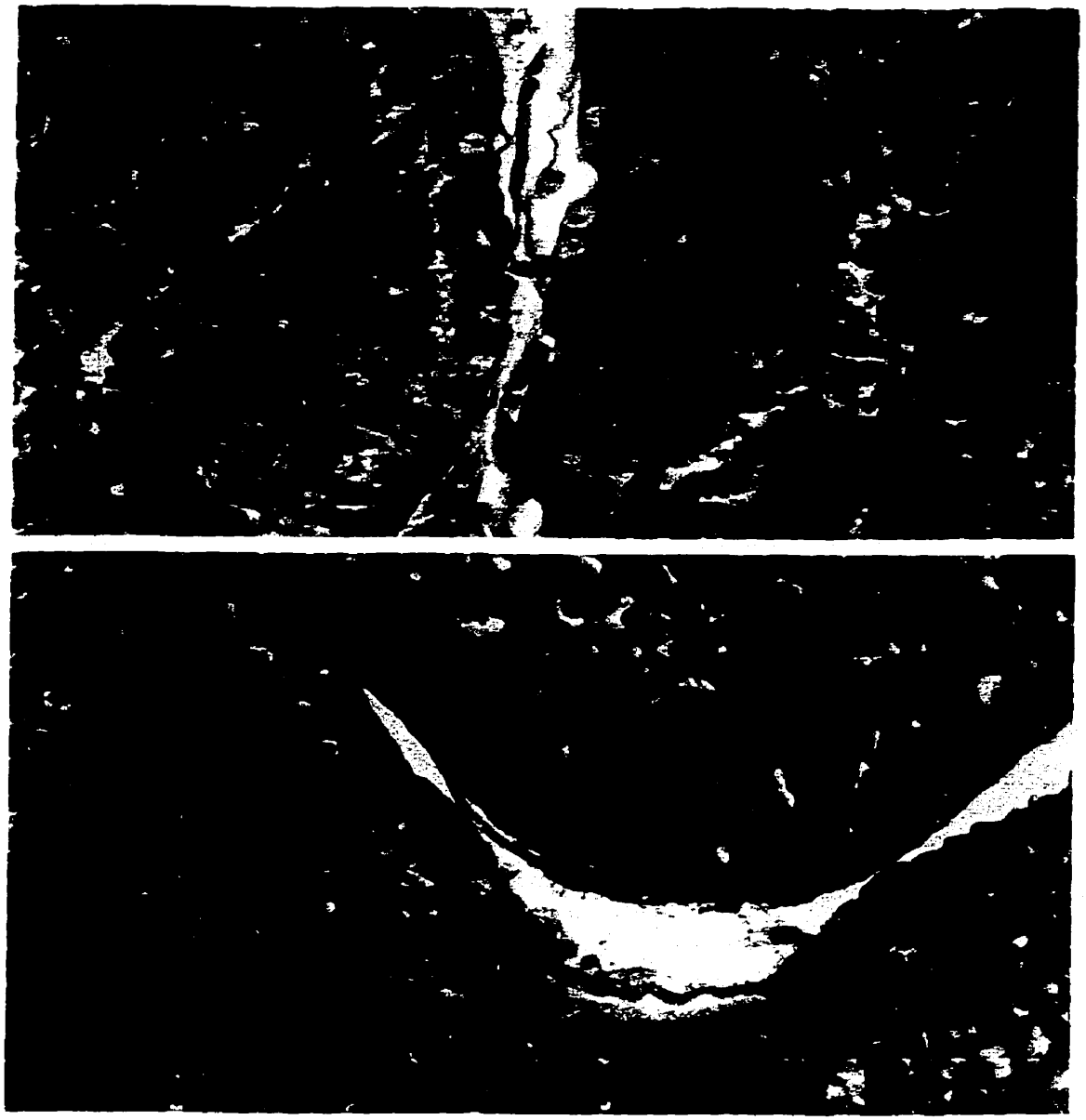

FIGURE 2 – Immunoperoxidase staining of *Bandicota indica* seminiferous tubules, using the ABC method. Both anti-bull PT and anti-PT 15 illustrated the same developmental pattern of labelling. **(a)** Anti-whole bull PT antibody (1449) strictly labels the spermatid population (S). **(b)** Anti-PT 15 antibody (as well as anti-1449 – not shown) illustrates initial labelling as it surrounds the acrosomic vesicle from the beginning of spermiogenesis (arrowheads) and continues its association with the acrosome and nucleus during their morphological change (arrows). Bars = 10 μm.

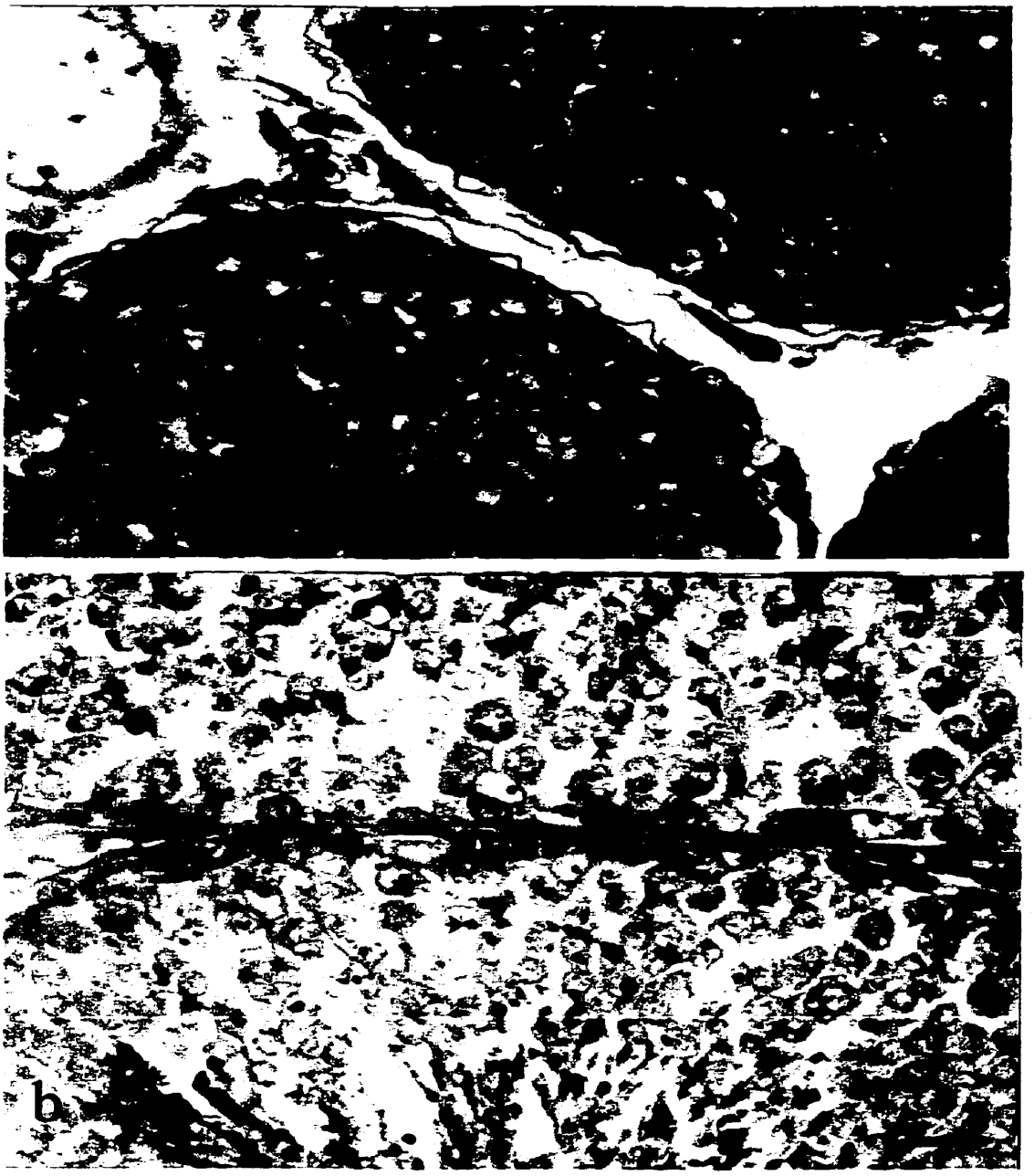
b

FIGURE 3 – Transmission Electron Micrograph of *Bandicota indica* sperm head epididymal section. Note the unusual sperm head morphology of this Southeast Asian rodent which is bulbous or globular in shape; it is atypical of the falciform shaped sperm heads of other rodents such as the lab rat, lab mouse and the Plains rat. Bar = 0.2 μm.


A